In response to EUMETSAT Invitation Tender ITT 22/224312

An update on the use of GRUAN sondes for the vicarious calibration of satellite microwave observations: the VICIRS study

CNR-IMAA: Elisabetta Ricciardelli, Domenico Cimini, Francesco Di Paola, Donatello Gallucci, Sabrina Gentile, Salvatore Larosa, Filomena Romano, Marco Rosoldi, Mariassunta Viggiano

Univ. Salerno: Fabio Madonna

In kind contributions:

Univ. Bergamo: Alessandro Fassò

MetOffice: Fabien Carminati

EUMETSAT: Francesco De Angelis, Vinia Mattioli, Tim Hewison, Axel Von Engeln

Aims

Develop a SW tool for vicarious calibration of MWI and ICI

- **Vicarious calibration**: post-launch calibration based on reference targets
  - E.g., other sat observations (well calibrated)
  - Simulated observations from radiosonde

- **MWI**: MicroWave Imager
- **ICI**: Ice Cloud Imager
  - To be launched with MetOp-SG-B (2026+)

- **GMI**: Global Precip Mission Microwave Imager
  - Currently in orbit with NASA GPM core

Aims

INPUT

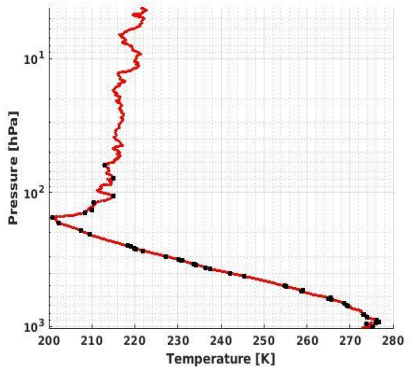

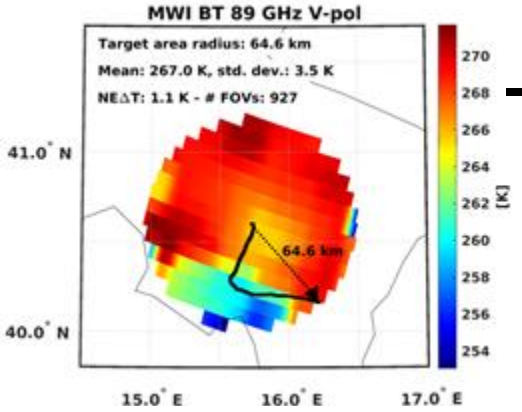

VICIRS TOOL

OUTPUT

BIAS & UNCERTAINTY

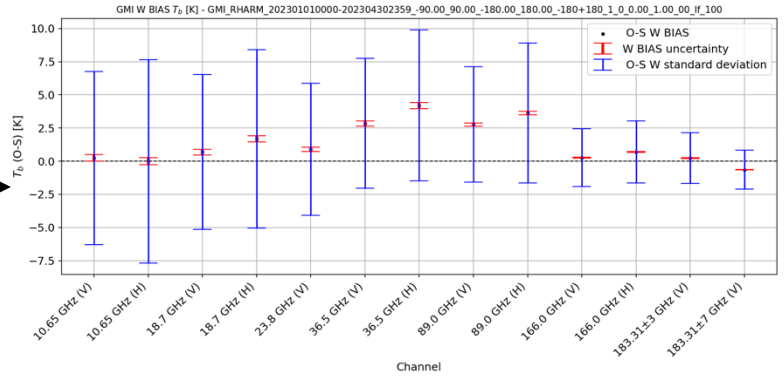

CHANNEL

Radiosondes

- Need for RS uncertainty

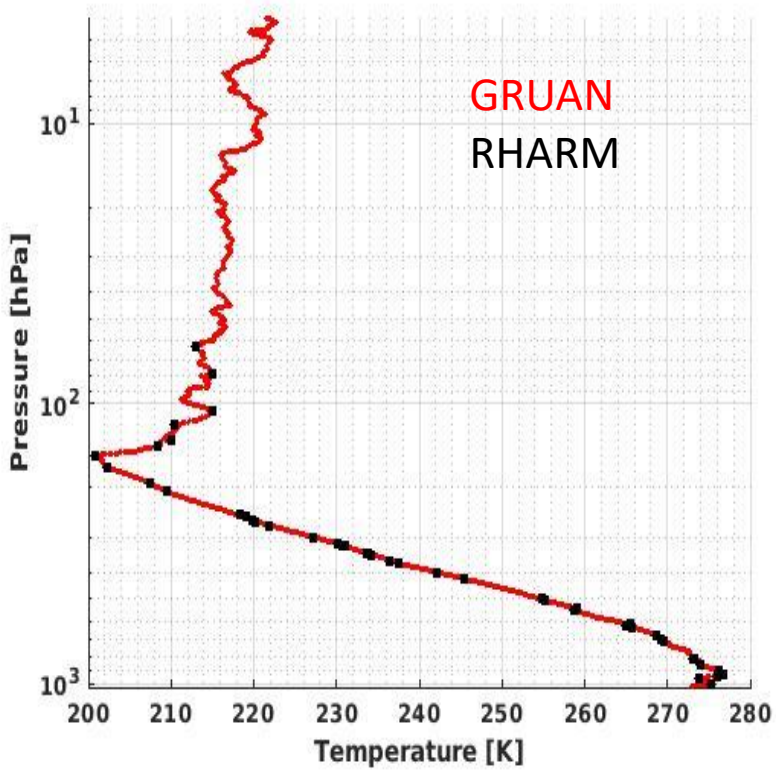

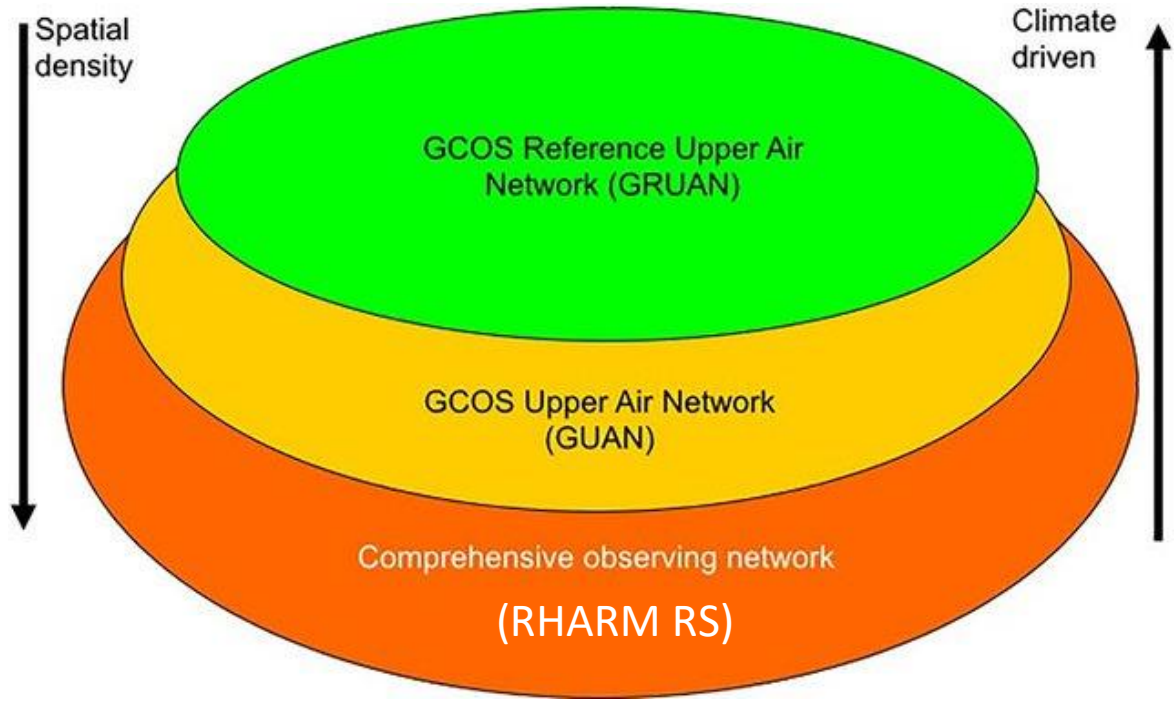

GCOS tiered-network concept

Radiosounding HARMonization (RHARM)

Copernicus Climate Change Service (C3S) - (Madonna et al, 2022)

- Builds on Integrated Global Radiosonde Archive (IGRA)
- bias-adjusted & estimated uncertainties
  - based on **GRUAN expertise and intercomparison** data
- 700 sites

- Now at RHARM v2

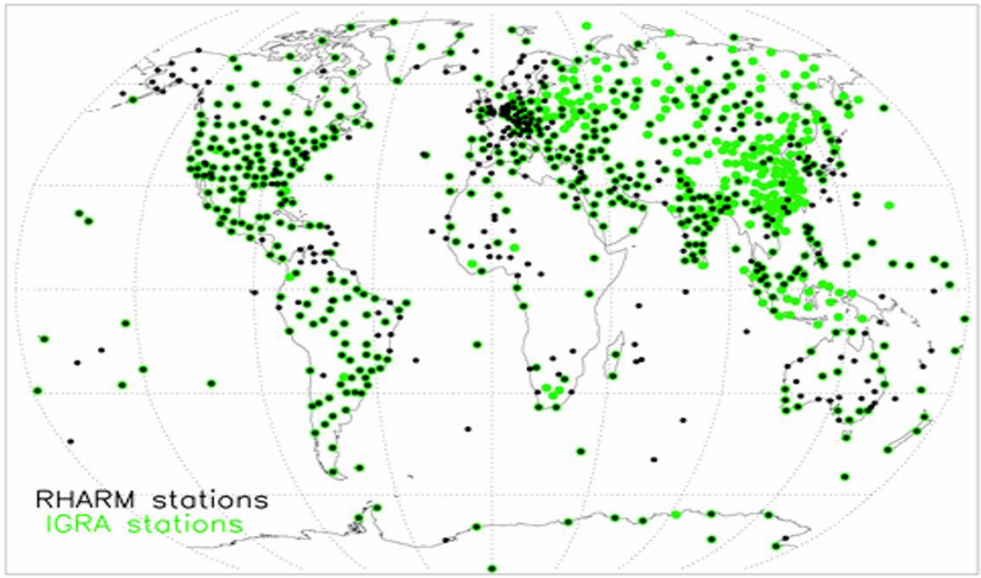

Uncertainty analysis

- Total uncertainty

$$u_{all} = \sqrt{\sum u_i^2} = \sqrt{u_{i_{OBS}}^2 + u_{i_{SIM}}^2 + u_{i_{COL}}^2}$$

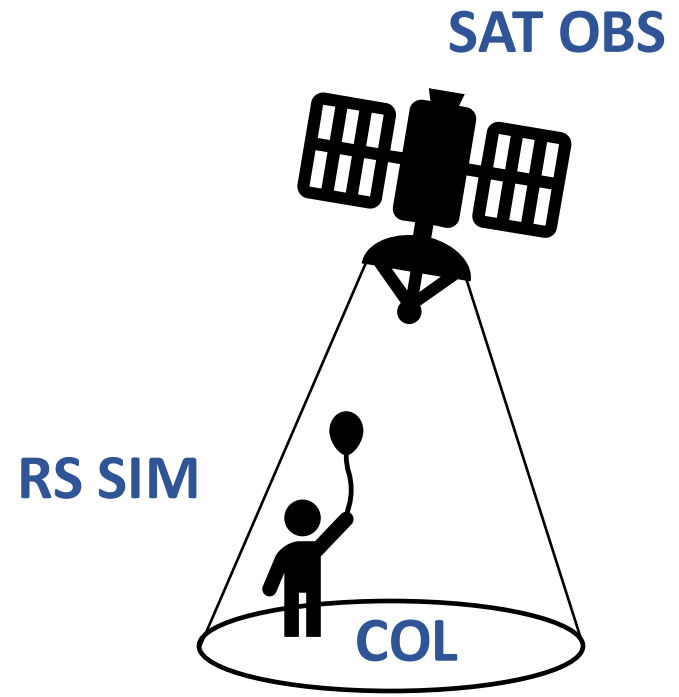

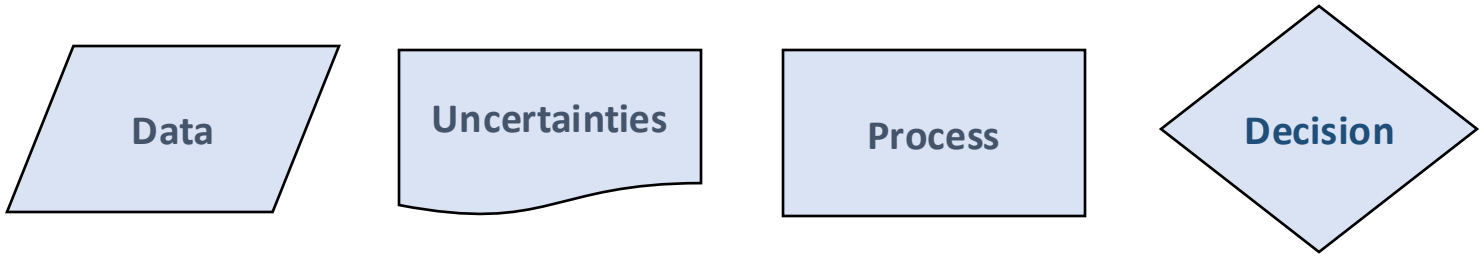

Uncertainty model diagram

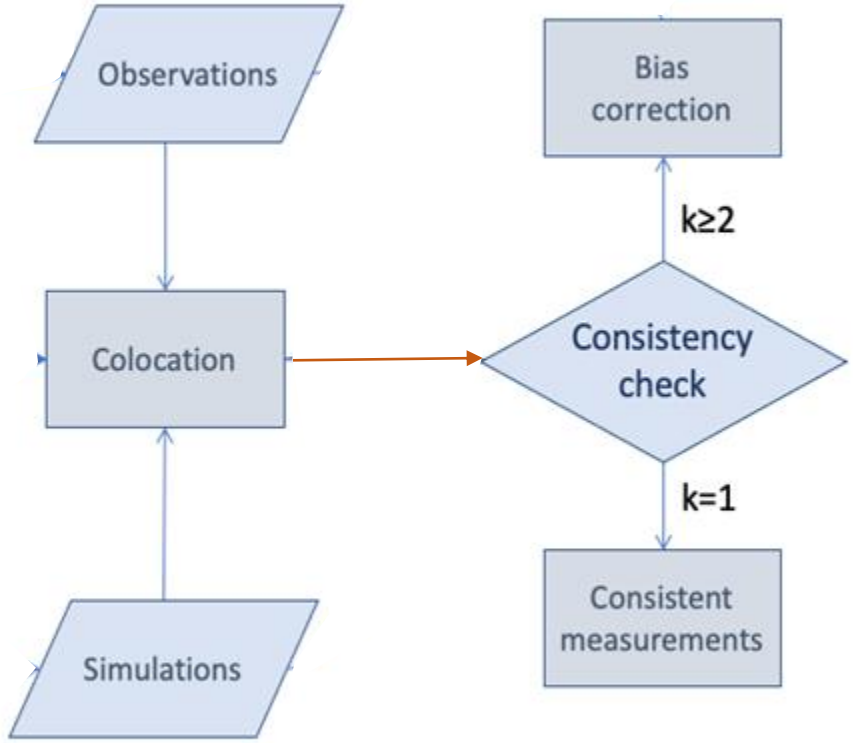

Uncertainty model diagram

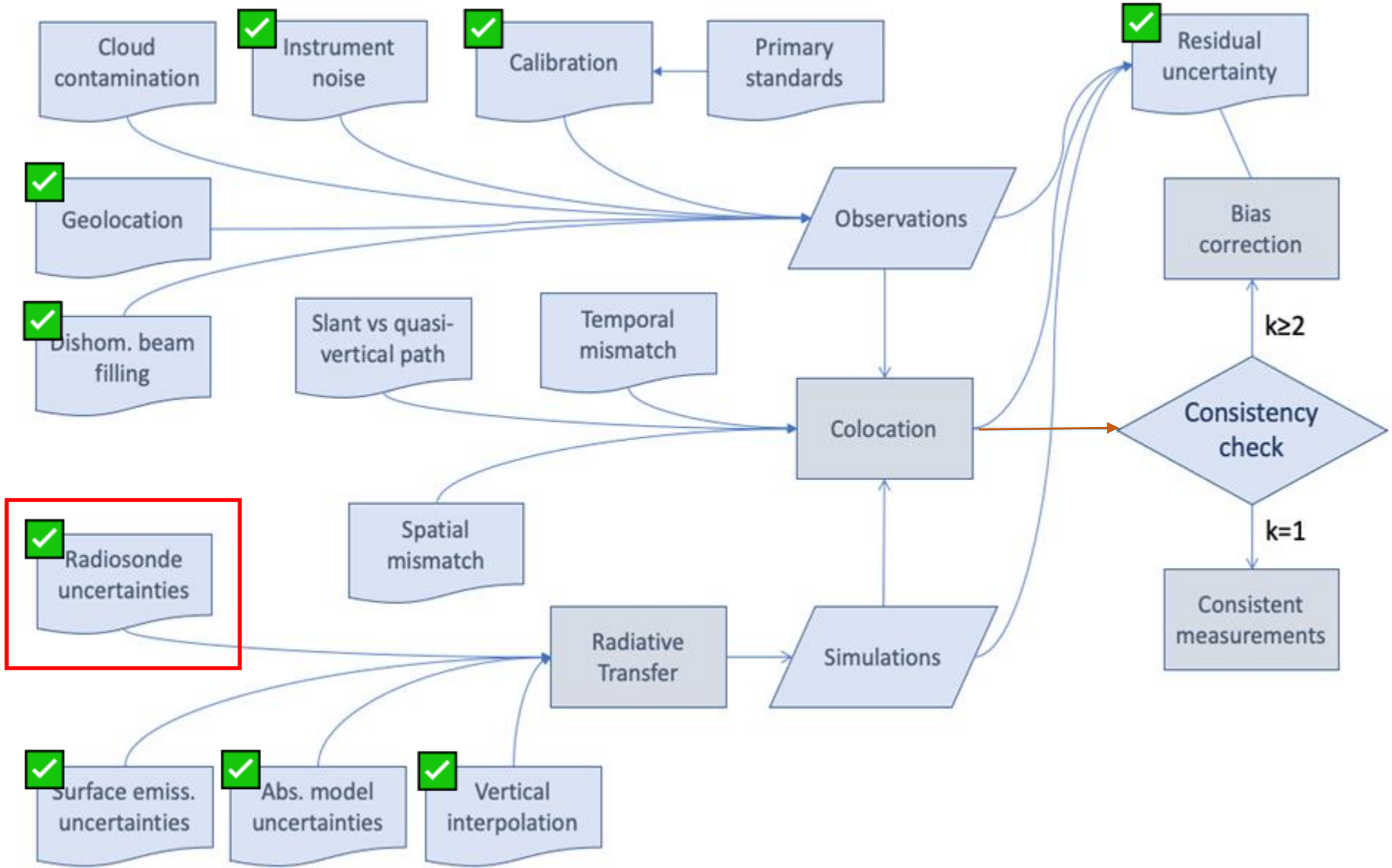

Propagating GDP uncertainty into RT

- Radiative transfer (RT) is performed through GRUAN processor (GPROC)
  - Initially developed within GAIA-CLIM
  - Updated within VICIRS (now at v6.3.b.0.3)

$$u\_BT_{RS} = \sqrt{KU^{RS}K^{T}} \text{ (diagonal terms)}$$

$$\begin{aligned} KU^{RS}K^{T} &= K_T \cdot U_T \cdot K_T^T + K_P \cdot U_P \cdot K_P^T + K_q \cdot U_q \cdot K_q^T \\ &+ K_{T2} \cdot U_{T2}^2 \cdot K_{T2}^T \\ &+ K_{q2} \cdot U_{q2}^2 \cdot K_{q2}^T + K_{Psurf} \cdot U_{Psurf}^2 \cdot K_{Psurf}^T \\ &+ K_{Tskin} \cdot U_{Tskin}^2 \cdot K_{Tskin}^T \end{aligned}$$

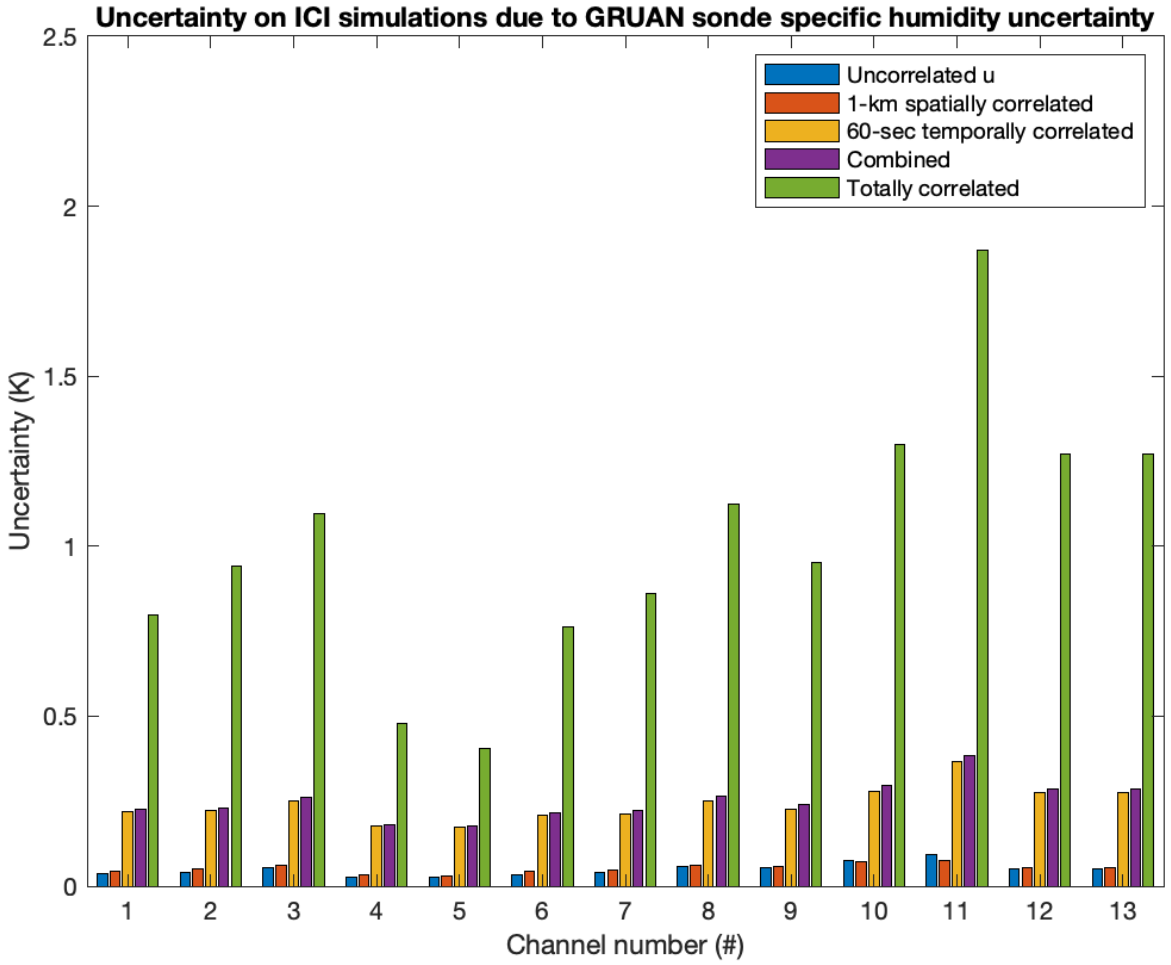

Uncertainty model diagram

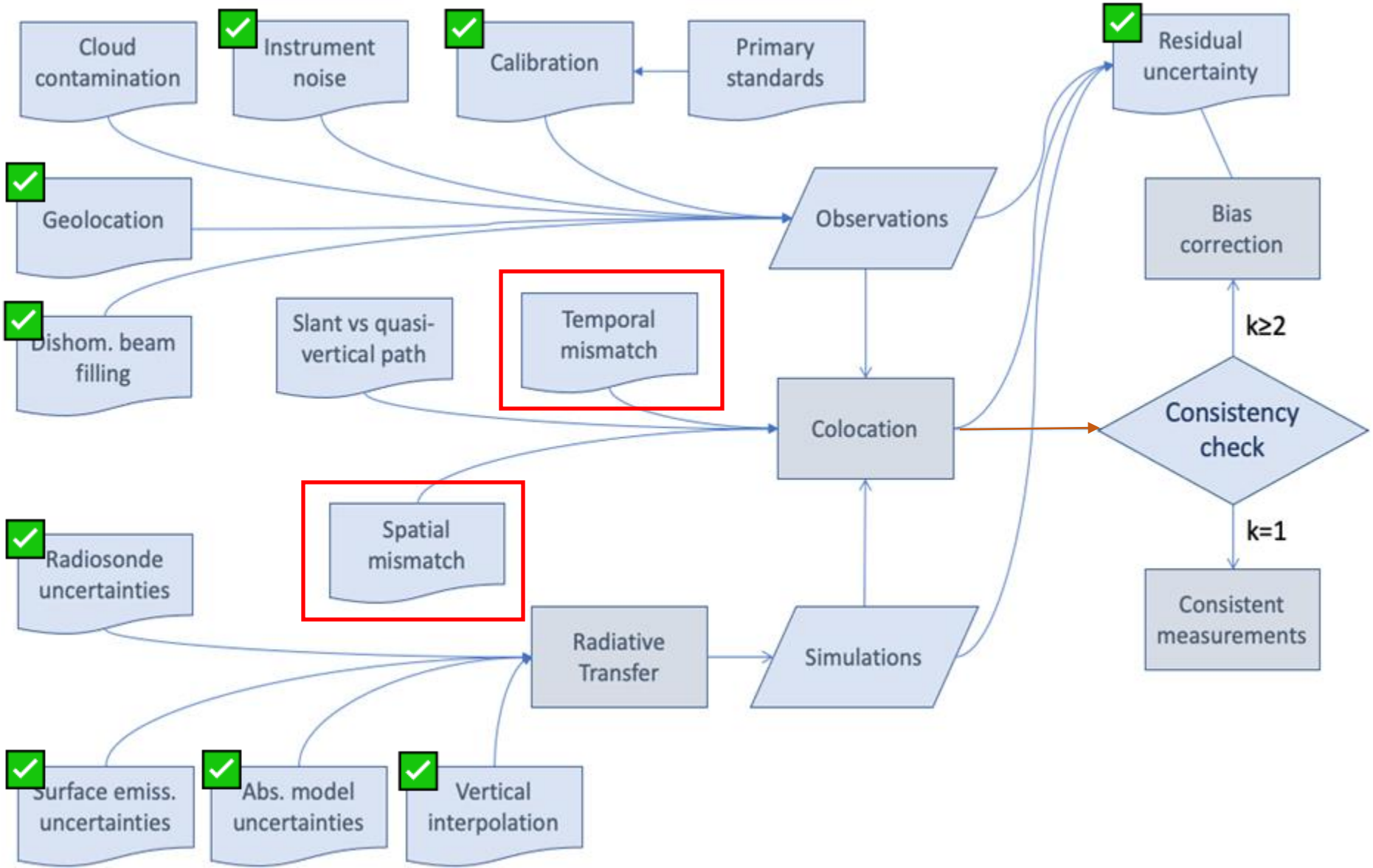

Knowledge gap analysis

Spatial & temporal RS representativeness:

- How RS measurements are representative for the spatial & temporal mismatch between the drifting point measurements and the satellite target area?

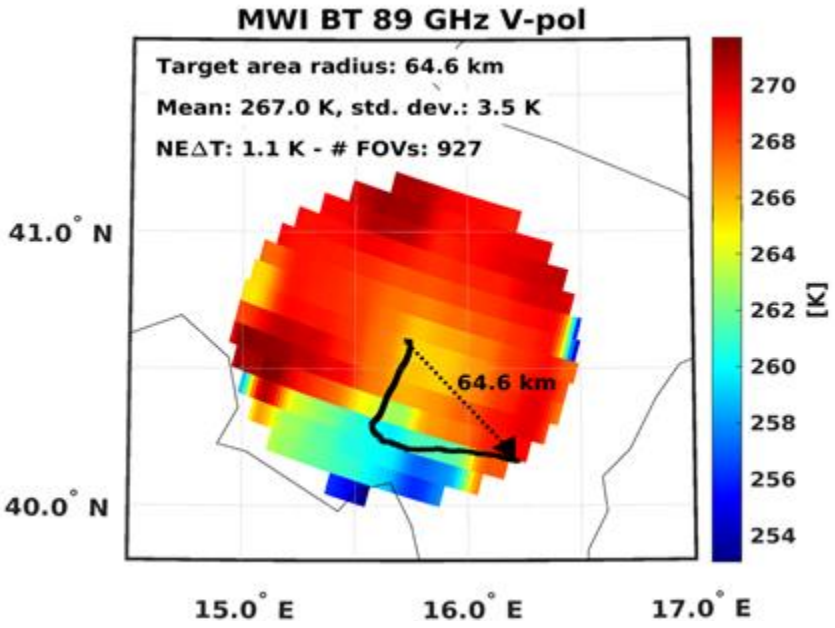

Spatial & temporal RS representativeness

Statistical approach

- Following Calbet et al., 2018; 2022
  - T & H structure functions (S)
    - Closely related to spatial auto-correlation
    - Derived from sequential sondes
  - Found 4 ranges
    - d < 2 km; 2 < d < 6 km; 6 < d < 10 km; d > 10 km

- S is related to field covariance as:
  - $S(r) = 2C(0) - 2C(r)$

- The excess covarience due to displacement *r*:
  - $EC(r) = C(0) - C(r) = 1/2\ S(r)$

- Assumption: *S* depends on horizontal distance *r* similarly at any height

- From lat/lon → distance → $EC_T(r)$ & $EC_e(r)$ → σ_T(h) & σ_e(h) → σ_{BT}

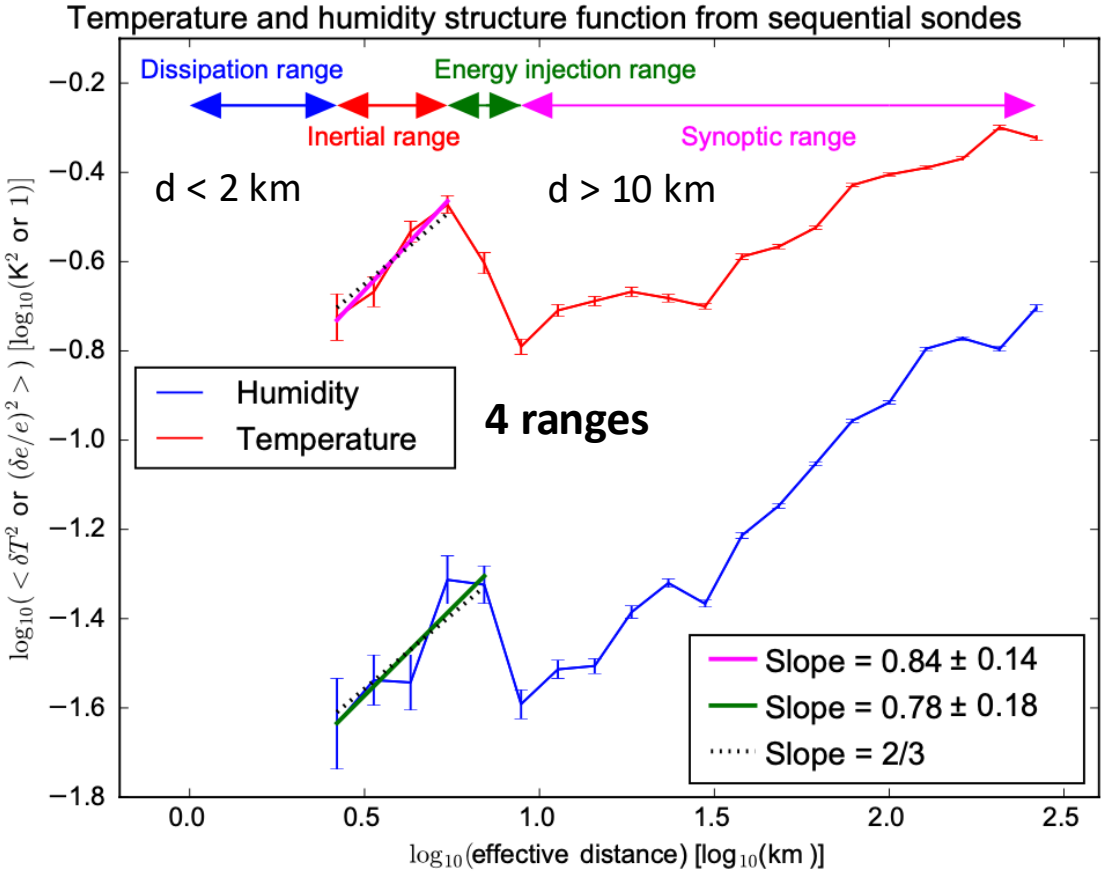

Spatial & temporal RS representativeness

NWP approach

- 4-D NWP fields are retrieved for each RS (lat, lon, height, time)
  - Lat-lon grid: 17-by-17 grid points
  - ~170x170 km around launch site
  - Time grid: 16 steps (before/after launch)

- BT is computed for each channel, grid point and time step (offline)
  - Investigate correlation between σ_{BT} and NWP proxies (e.g. T_{skin}, TCWV, K,…)
  - Train a simple model to estimate σ_{BT} from most relevant proxies

TCWV

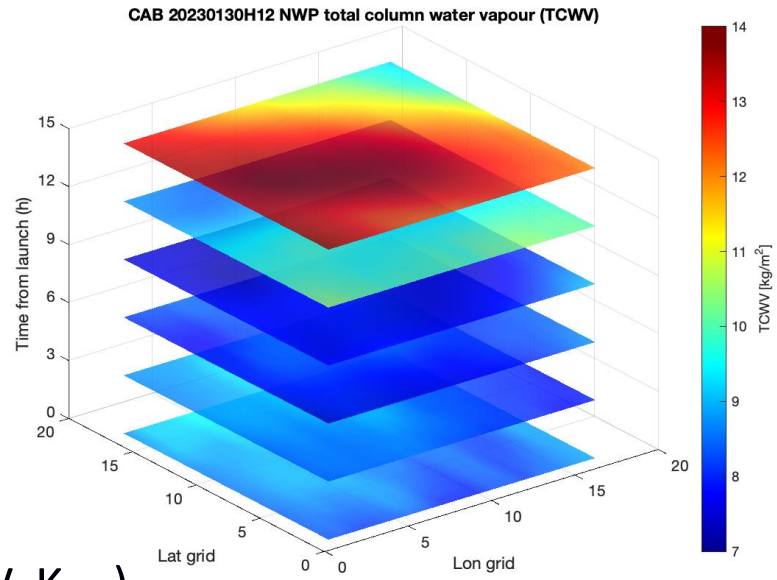

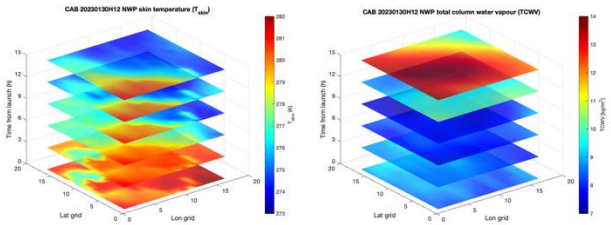

σ_{BT} → Relate σ_{BT} to σ_{proxy}

Spatial RS representativeness

GMI channels (13)

No.	Central frequency (GHz)	Bandwidth (MHz)	Polarisation	NEΔT	IFOV	Pixel
1	10.65	100	V	0.96 K	19x32 km	12x13.4 km
2	10.65	100	H	0.96 K	19x32 km	12x13.4 km
3	18.7	200	V	0.84 K	11x18 km	6.0x13.4 km
4	18.7	200	H	0.84 K	11x18 km	6.0x13.4 km
5	23.8	400	V	1.05 K	9.2x15 km	6.0x13.4 km
6	36.5	1000	V	0.65 K	8.6x14 km	6.0x13.4 km
7	36.5	1000	H	0.65 K	8.6x14 km	6.0x13.4 km
8	89.0	6000	V	0.57 K	4.4x7.2 km	3.0x13.4 km
9	89.0	6000	H	0.57 K	4.4x7.2 km	3.0x13.4 km
10	166.5	4000	V	1.5 K	4.4x7.2 km	3.0x13.4 km
11	166.5	4000	H	1.5 K	4.4x7.2 km	3.0x13.4 km
13	183.31 ± 7	2000	V	1.5 K	4.4x7.2 km	3.0x13.4 km
12	183.31 ± 3	2000	V	1.5 K	4.4x7.2 km	3.0x13.4 km

BT spatial variability from NWP (13 GMI channels)

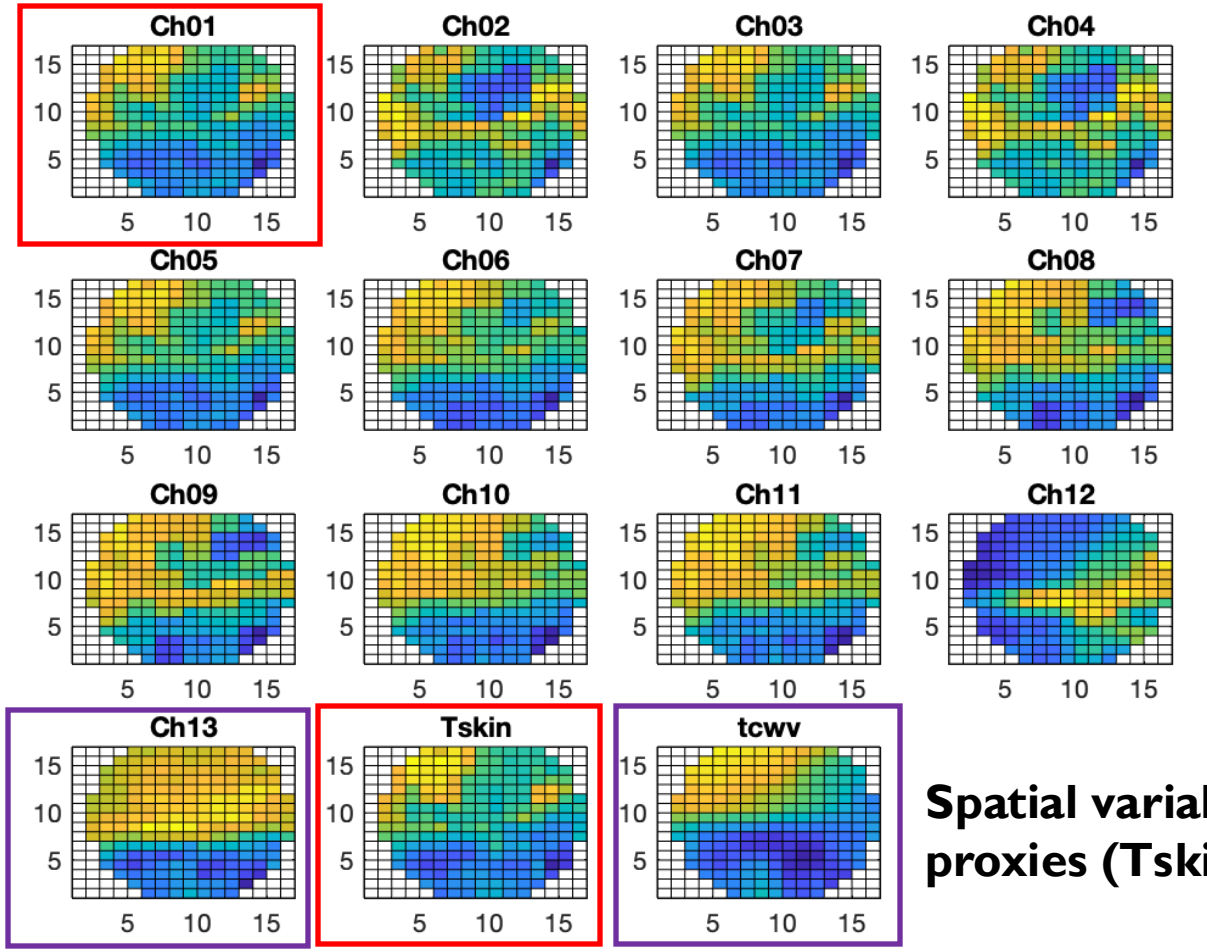

WORK IN PROGRESS

Spatial variability of NWP proxies (Tskin, tcwv)

Spatial RS representativeness

σ_{proxy} → σ_{BT}

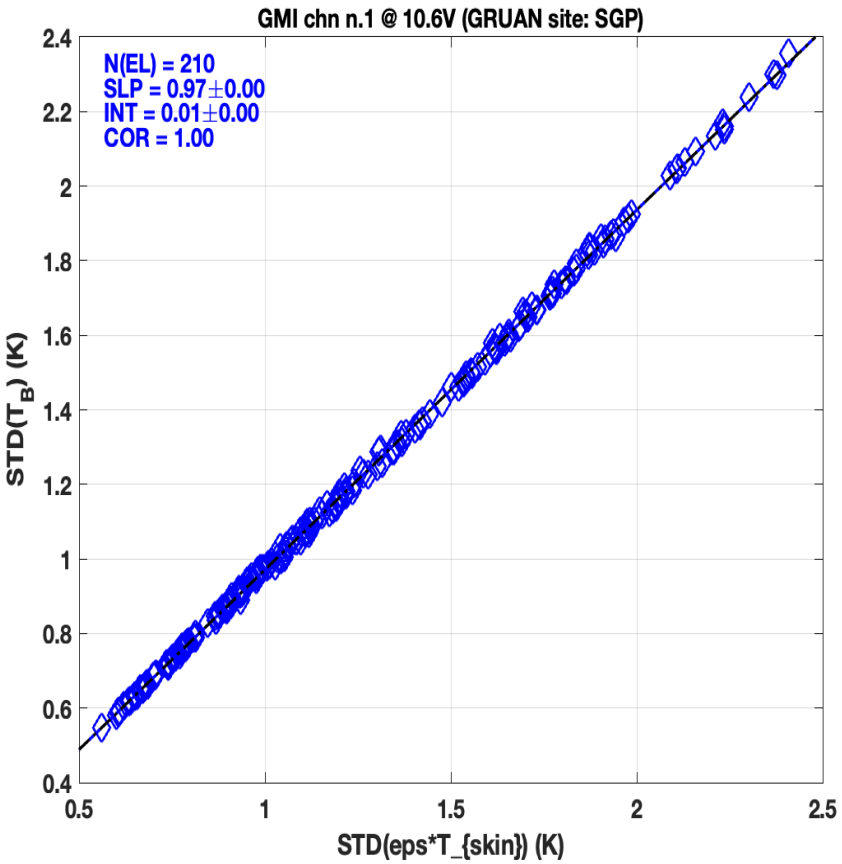

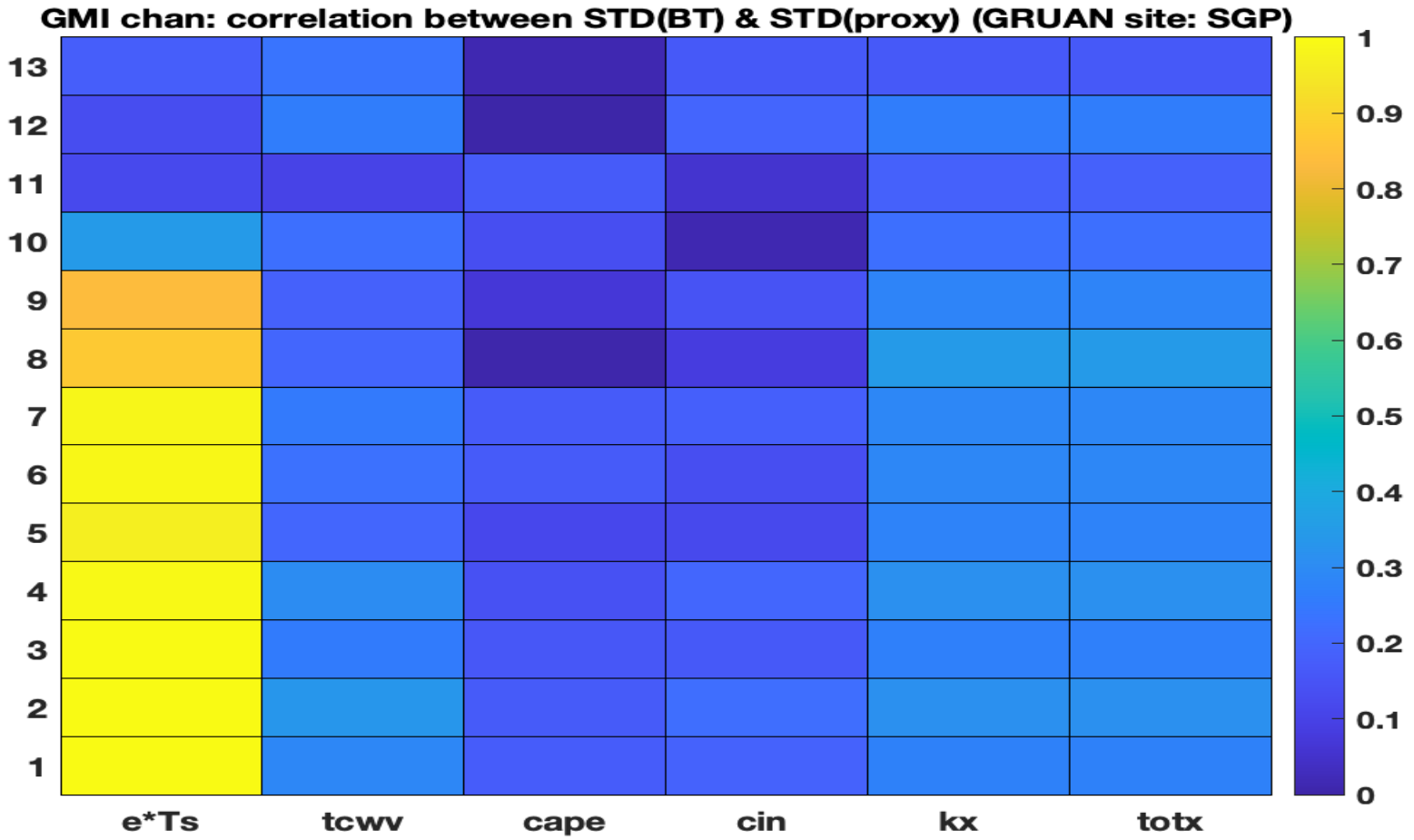

Temporal RS representativeness

No.	Central frequency (GHz)	Bandwidth (MHz)	Polarisation	NEΔT	IFOV	Pixel
1	10.65	100	V	0.96 K	19x32 km	12x13.4 km
2	10.65	100	H	0.96 K	19x32 km	12x13.4 km
3	18.7	200	V	0.84 K	11x18 km	6.0x13.4 km
4	18.7	200	H	0.84 K	11x18 km	6.0x13.4 km
5	23.8	400	V	1.05 K	9.2x15 km	6.0x13.4 km
6	36.5	1000	V	0.65 K	8.6x14 km	6.0x13.4 km
7	36.5	1000	H	0.65 K	8.6x14 km	6.0x13.4 km
8	89.0	6000	V	0.57 K	4.4x7.2 km	3.0x13.4 km
9	89.0	6000	H	0.57 K	4.4x7.2 km	3.0x13.4 km
10	166.5	4000	V	1.5 K	4.4x7.2 km	3.0x13.4 km
11	166.5	4000	H	1.5 K	4.4x7.2 km	3.0x13.4 km
13	183.31 ± 7	2000	V	1.5 K	4.4x7.2 km	3.0x13.4 km
12	183.31 ± 3	2000	V	1.5 K	4.4x7.2 km	3.0x13.4 km

BT temporal variability from NWP (13 GMI channels)

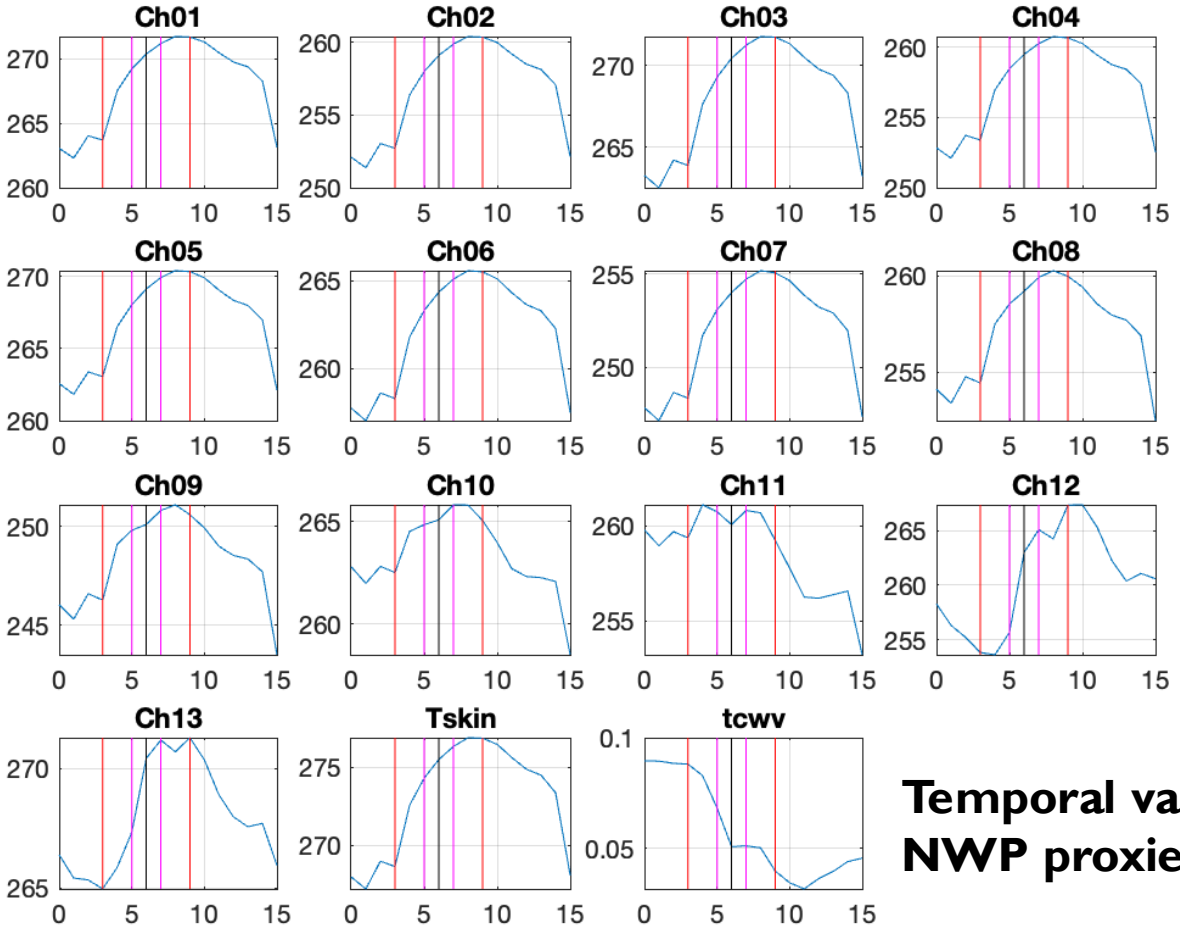

WORK IN PROGRESS

Temporal variability of NWP proxies (Tskin, tcwv)

Analysis on GRUAN dedicated launches

- Dedicated launches (DL) will be performed during the MWI/ICI validation campaign (EUMETSAT)

- Sites for DL may be selected according to:
  - spatial distribution of GRUAN sites
  - number of Metop-SGB–GRUAN colocation match-ups (MU)
  - coverage of different climate regimes

Code	Name	Lat	Lon	Alt (m)	Lat zone	NWS	RS lanches in 2022 (type)
ALC	Alice Springs, Australia	-23.79°	133.89°	546	TROP	X	—
BAR	Barrow, AK, USA	71.32°	-156.61°	8	POLA	X	1350 (RS-41)
BEL	Beltsville, MD, USA	39.05°	-76.88°	53	MIDL		62 (RS-41)
BOU	Boulder, CO, USA	39.95°	-105.20°	1743	MIDL		46 (RS-41)
CAB	Cabauw, Netherlands	51.97°	4.92°	1	MIDL	X	62 (RS-41)
DAK	Dakar, Senegal	14.73°	-17.50°	25	TROP		—
DAR	Darwin, Australia	-12.43°	130.89°	30	TROP	X	—
DVS	Davis, Antarctica (AU)	-68.57°	77.97°	18	POLA	X	—
DLG	Dolgoprudny, Russia	55.56°	37.52°	185	MIDL		—
GRA	Graciosa, Portugal	39.09°	-28.03°	30	MIDL	X	770 (RS-41)
GVN	Neumayer, Antarctica (DE)	-70.65°	-8.25°	43	POLA	X	363 (RS-41)
HKO	Hong Kong, China	22.30°	114.17°	32	TROP	X	354 (RS-41)
LAU	Lauder, New Zealand	-45.05°	169.68°	370	MIDL	X	826 (RS-41)
LIN	Lindenberg, Germany	52.21°	14.12°	98	MIDL	X	1601 (RS-41) - 95 (IMS-100)
MAQ	Macquarie Island, Australia	-54.50°	158.94°	6	MIDL	X	—
MAN	Manus, Papua New Guinea	-2.06°	147.42°	6	TROP		inactive
MEL	Melbourne, Australia	-37.67°	144.83°	113	MIDL	X	—
MTS	Minamitorishima, Japan	24.29°	153.98°	9	TROP	X	728 (IMS-100)
NAU	Nauru, Nauru	-0.52°	166.92°	7	TROP		inactive
NYA	Ny-Ålesund, Svalbard(DE, FR)	78.92°	11.93°	5	POLA	X	—
PAY	Payerne, Switzerland	46.81°	6.95°	491	MIDL	X	745 (RS-41)
PMO	Paramaribo, Suriname	5.81°	-55.21°	4	TROP		66 (RS-41)
POT	Potenza, Italy	40.60°	15.72°	720	MIDL		82 (RS-41)
REU	La Réunion, France	-20.89°	55.49°	13 - 2200	TROP	X	—
ROS	Ross Island, Antarctica (NZ, US)	-77.85°	166.65°	10 - 200	POLA	X	517 (RS-41)
SGP	Lamont, OK, USA	36.60°	-97.49°	320	MIDL	X	636 (RS-41)
SNG	Singapore, Singapore	1.30°	103.80°	21	TROP	X	17 (RS-41) - 649 (IMS-100)
SOD	Sodankylä, Finland	67.37°	26.63°	179	POLA	X	752 (RS-41)
SYO	Syowa, Antarctica (JP)	-69.00°	39.58°	22	POLA	X	6 (IMS-100) - 686 (RS-11G)
TAT	Tateno, Japan	36.06°	140.13°	27	TROP	X	340 (RS-41) - 144 (IMS-100) - 2 (RS-11G)
TEN	Tenerife, Spain	28.32°	-16.38°	115	TROP	X	755 (RS-41)
TRP	Trappes Palaiseau, France	48.7°	2.2°	156	MIDL	X	—
XIL	Xilin Hot, China	43.95°	116.12°	1013	MIDL		—

Grey: No GDPs available

Code	Name	Lat	Lon	Alt (m)	Lat zone	NWS	RS lanches in 2022 (type)
ALC	Alice Springs, Australia	-23.79°	133.89°	546	TROP	X	—
BAR	Barrow, AK, USA	71.32°	-156.61°	8	POLA	X	1350 (RS-41)
BEL	Beltsville, MD, USA	39.05°	-76.88°	53	MIDL		62 (RS-41)
BOU	Boulder, CO, USA	39.95°	-105.20°	1743	MIDL		46 (RS-41)
CAB	Cabauw, Netherlands	51.97°	4.92°	1	MIDL	X	62 (RS-41)
DAK	Dakar, Senegal	14.73°	-17.50°	25	TROP		—
DAR	Darwin, Australia	-12.43°	130.89°	30	TROP	X	—
DVS	Davis, Antarctica (AU)	-68.57°	77.97°	18	POLA	X	—
DLG	Dolgoprudny, Russia	55.56°	37.52°	185	MIDL		—
GRA	Graciosa, Portugal	39.09°	-28.03°	30	MIDL	X	770 (RS-41)
GVN	Neumayer, Antarctica (DE)	-70.65°	-8.25°	43	POLA	X	363 (RS-41)
HKO	Hong Kong, China	22.30°	114.17°	32	TROP	X	354 (RS-41)
LAU	Lauder, New Zealand	-45.05°	169.68°	370	MIDL	X	826 (RS-41)
LIN	Lindenberg, Germany	52.21°	14.12°	98	MIDL	X	1601 (RS-41) - 95 (IMS-100)
MAQ	Macquarie Island, Australia	-54.50°	158.94°	6	MIDL	X	—
MAN	Manus, Papua New Guinea	-2.06°	147.42°	6	TROP		inactive
MEL	Melbourne, Australia	-37.67°	144.83°	113	MIDL	X	—
MTS	Minamitorishima, Japan	24.29°	153.98°	9	TROP	X	728 (IMS-100)
NAU	Nauru, Nauru	-0.52°	166.92°	7	TROP		inactive
NYA	Ny-Ålesund, Svalbard(DE, FR)	78.92°	11.93°	5	POLA	X	—
PAY	Payerne, Switzerland	46.81°	6.95°	491	MIDL	X	745 (RS-41)
PMO	Paramaribo, Suriname	5.81°	-55.21°	4	TROP		66 (RS-41)
POT	Potenza, Italy	40.60°	15.72°	720	MIDL		82 (RS-41)
REU	La Réunion, France	-20.89°	55.49°	13 - 2200	TROP	X	—
ROS	Ross Island, Antarctica (NZ, US)	-77.85°	166.65°	10 - 200	POLA	X	517 (RS-41)
SGP	Lamont, OK, USA	36.60°	-97.49°	320	MIDL	X	636 (RS-41)
SNG	Singapore, Singapore	1.30°	103.80°	21	TROP	X	17 (RS-41) - 649 (IMS-100)
SOD	Sodankylä, Finland	67.37°	26.63°	179	POLA	X	752 (RS-41)
SYO	Syowa, Antarctica (JP)	-69.00°	39.58°	22	POLA	X	6 (IMS-100) - 686 (RS-11G)
TAT	Tateno, Japan	36.06°	140.13°	27	TROP	X	340 (RS-41) - 144 (IMS-100) - 2 (RS-11G)
TEN	Tenerife, Spain	28.32°	-16.38°	115	TROP	X	755 (RS-41)
TRP	Trappes Palaiseau, France	48.7°	2.2°	156	MIDL	X	—
XIL	Xilin Hot, China	43.95°	116.12°	1013	MIDL		—

Blue: GRUAN sites not involved with the validation campaign but performing regular launches

Code	Name	Lat	Lon	Alt (m)	Lat zone	NWS	RS lanches in 2022 (type)
ALC	Alice Springs, Australia	-23.79°	133.89°	546	TROP	X	—
BAR	Barrow, AK, USA	71.32°	-156.61°	8	POLA	X	1350 (RS-41)
BEL	Beltsville, MD, USA	39.05°	-76.88°	53	MIDL		62 (RS-41)
BOU	Boulder, CO, USA	39.95°	-105.20°	1743	MIDL		46 (RS-41)
CAB	Cabauw, Netherlands	51.97°	4.92°	1	MIDL	X	62 (RS-41)
DAK	Dakar, Senegal	14.73°	-17.50°	25	TROP		—
DAR	Darwin, Australia	-12.43°	130.89°	30	TROP	X	—
DVS	Davis, Antarctica (AU)	-68.57°	77.97°	18	POLA	X	—
DLG	Dolgoprudny, Russia	55.56°	37.52°	185	MIDL		—
GRA	Graciosa, Portugal	39.09°	-28.03°	30	MIDL	X	770 (RS-41)
GVN	Neumayer, Antarctica (DE)	-70.65°	-8.25°	43	POLA	X	363 (RS-41)
HKO	Hong Kong, China	22.30°	114.17°	32	TROP	X	354 (RS-41)
LAU	Lauder, New Zealand	-45.05°	169.68°	370	MIDL	X	826 (RS-41)
LIN	Lindenberg, Germany	52.21°	14.12°	98	MIDL	X	1601 (RS-41) - 95 (IMS-100)
MAQ	Macquarie Island, Australia	-54.50°	158.94°	6	MIDL	X	—
MAN	Manus, Papua New Guinea	-2.06°	147.42°	6	TROP		inactive
MEL	Melbourne, Australia	-37.67°	144.83°	113	MIDL	X	—
MTS	Minamitorishima, Japan	24.29°	153.98°	9	TROP	X	728 (IMS-100)
NAU	Nauru, Nauru	-0.52°	166.92°	7	TROP		inactive
NYA	Ny-Ålesund, Svalbard(DE, FR)	78.92°	11.93°	5	POLA	X	—
PAY	Payerne, Switzerland	46.81°	6.95°	491	MIDL	X	745 (RS-41)
PMO	Paramaribo, Suriname	5.81°	-55.21°	4	TROP		66 (RS-41)
POT	Potenza, Italy	40.60°	15.72°	720	MIDL		82 (RS-41)
REU	La Réunion, France	-20.89°	55.49°	13 - 2200	TROP	X	—
ROS	Ross Island, Antarctica (NZ, US)	-77.85°	166.65°	10 - 200	POLA	X	517 (RS-41)
SGP	Lamont, OK, USA	36.60°	-97.49°	320	MIDL	X	636 (RS-41)
SNG	Singapore, Singapore	1.30°	103.80°	21	TROP	X	17 (RS-41) - 649 (IMS-100)
SOD	Sodankylä, Finland	67.37°	26.63°	179	POLA	X	752 (RS-41)
SYO	Syowa, Antarctica (JP)	-69.00°	39.58°	22	POLA	X	6 (IMS-100) - 686 (RS-11G)
TAT	Tateno, Japan	36.06°	140.13°	27	TROP	X	340 (RS-41) - 144 (IMS-100) - 2 (RS-11G)
TEN	Tenerife, Spain	28.32°	-16.38°	115	TROP	X	755 (RS-41)
TRP	Trappes Palaiseau, France	48.7°	2.2°	156	MIDL	X	—
XIL	Xilin Hot, China	43.95°	116.12°	1013	MIDL		—

GRUAN sites involved with the validation campaign

Code	Name	Lat	Lon	Alt (m)	Lat zone	NWS	RS lanches in 2022 (type)
CAB	Cabauw, Netherlands	51.97°	4.92°	1	MIDL	X	62 (RS-41)
LAU	Lauder, New Zealand	-45.05°	169.68°	370	MIDL	X	826 (RS-41)
LIN	Lindenberg, Germany	52.21°	14.12°	98	MIDL	X	1601 (RS-41) - 95 (IMS-100)
PAY	Payerne, Switzerland	46.81°	6.95°	491	MIDL	X	745 (RS-41)
PMO	Paramaribo, Suriname	5.81°	-55.21°	4	TROP		66 (RS-41)
POT	Potenza, Italy	40.60°	15.72°	720	MIDL		82 (RS-41)
SOD	Sodankylä, Finland	67.37°	26.63°	179	POLA	X	752 (RS-41)
TAT	Tateno, Japan	36.06°	140.13°	27	TROP	X	340 (RS-41) - 144 (IMS-100) - 2 (RS-11G)
TEN	Tenerife, Spain	28.32°	-16.38°	115	TROP	X	755 (RS-41)
XIL	Xilin Hot, China	43.95°	116.12°	1013	MIDL		—

Analysis on GRUAN dedicated launches

For 1-year (2022)

GRUAN sites involved with the validation campaign: MU stats for +/-3h window

Code	Name	Lat zone	RS launches in 2022	3h-MU (#)	3h-MU unique (#)	Cloudy (RS-test)	Clear (RS-test)	RS-test (%)	Usable MU (*)
CAB	Cabauw	MIDL	62	7	7	7	0	100,0	0
LAU	Lauder	MIDL	826	627	624	440	184	70,5	112
LIN	Lindenberg	MIDL	1702	790	749	432	317	57,7	193
PAY	Payerne	MIDL	745	271	267	138	129	51,7	79
PMO	Paramaribo	TROP	66	18	17	14	3	82,4	2
POT	Potenza	MIDL	88	40	40	0	40	0,0	24
SOD	Sodankylä	POLA	752	498	388	289	99	74,5	60
TAT	Tateno	TROP	484	326	323	140	183	43,3	112
TEN	Tenerife	TROP	755	481	479	175	304	36,5	185
XIL	Xilin Hot	MIDL	0	0	0	0	0	--	0
TOT			**5480**	**3058**	**2894**	**1635**	**1259**		**768**

SUMMARY & CONSIDERATIONS

- MIDL: MU>400 (LAU: 112, LIN: 193, PAY: 79, POT: 24) (ALL SITES: 553)
- TROP: MU~300 (PMO: 2, TAT: 112, TEN: 185) (ALL SITES: 504)
- POLA: MU~60 (SOD: 60) (ALL SITES: 633)
  - Other polar GRUAN sites contribute with additional >550MU
  - Not worth increasing launches with DL
- Suggestion: Assign DL to PMO & POT to increase statistical significance at these sites

(*) after TA-test, assuming 39% cloudy TA (mean for GMI)

Analysis on GRUAN dedicated launches

For 1-year (2022)

GRUAN sites involved with the validation campaign: MU stats for +/-1h window

Code	Name	Lat zone	RS launches in 2022	1h-MU (#)	1h-MU unique (#)	Cloudy (RS-test)	Clear (RS-test)	RS-test (%)	Usable MU (*)
CAB	Cabauw,	MIDL	62	0	0	0	0	--	0
LAU	Lauder	MIDL	826	444	443	317	126	71,6	77
LIN	Lindenberg	MIDL	1702	61	58	28	30	48,3	18
PAY	Payerne	MIDL	745	2	1	1	0	100,0	0
PMO	Paramaribo	TROP	66	0	0	0	0	--	0
POT	Potenza	MIDL	88	9	9	0	9	0,0	5
SOD	Sodankylä	POLA	752	56	54	33	21	61,1	13
TAT	Tateno	TROP	484	310	307	132	175	43,0	107
TEN	Tenerife	TROP	755	412	410	146	269	35,6	164
XIL	Xilin Hot	MIDL	0	0	0	0	0	--	0
TOT			**5480**	**1294**	**1282**	**657**	**630**		**384**

SUMMARY & CONSIDERATIONS

- MIDL: MU~100 (LAU: 77, LIN: 18, PAY: 0, POT: 5) (ALL SITES: 167)
- TROP: MU~270 (PMO: 0, TAT: 107, TEN: 164) (ALL SITES: 352)
- POLA: MU~13 (SOD: 13) (ALL SITES: 268)
  - Other polar GRUAN sites contribute with additional >250MU
  - Not worth increasing launches with DL
- Suggestion: Assign DL to PAY, POT, PMO, SOD to increase statistical significance at these sites

(*) after TA-test, assuming 39% cloudy TA (mean for GMI)

Analysis on GRUAN dedicated launches

For 1-year (2022)

GRUAN sites involved with the validation campaign: MU stats for -15'/+45' window

Code	Name	Lat zone	RS launches in 2022	1h-MU (#)	1h-MU unique (#)	Cloudy (RS-test)	Clear (RS-test)	RS-test (%)	Usable MU (*)
CAB	Cabauw,	MIDL	62	0	0	0	0	--	0
LAU	Lauder	MIDL	826	238	237	176	61	74,3	37
LIN	Lindenberg	MIDL	1702	19	17	6	11	35,3	7
PAY	Payerne	MIDL	745	0	0	0	0	--	0
PMO	Paramaribo	TROP	66	0	0	0	0	--	0
POT	Potenza	MIDL	88	4	4	0	4	0,0	2
SOD	Sodankylä	POLA	752	22	22	12	10	54,5	6
TAT	Tateno	TROP	484	178	175	48	105	27,4	64
TEN	Tenerife	TROP	755	317	315	115	200	36,5	122
XIL	Xilin Hot	MIDL	0	0	0		0	--	0
TOT			**5480**	**778**	**770**	**357**	**391**		**239**

SUMMARY & CONSIDERATIONS

- MIDL: MU~50 (LAU: 37, LIN: 7, PAY: 0, POT: 2) (ALL SITES: 78)
- TROP: MU~185 (PMO: 0, TAT: 64, TEN: 122) (ALL SITES: 244)
- POLA: MU~6 (SOD: 6) (ALL SITES: 146)
  - Other polar GRUAN sites contribute with additional >140MU
  - May be worth increasing launches with DL
- Suggestion: Assign DL to PAY, POT, LIN, SOD, PMO to increase statistical significance at these sites

(*) after TA-test, assuming 39% cloudy TA (mean for GMI)

Analysis on GRUAN dedicated launches

Summary (based on METOB-SGB/GRUAN MUs for 1 year, 2022)

Temporal MU criteria	DL assignment priority
3h	PMO, POT
1h	PAY, POT, PMO, SOD
-15'/+45'	PAY, POT, LIN, SOD, PMO

Analysis on GRUAN dedicated launches

Optimal launching time

Temporal distance between DL and satellite overpass

1. **Radiosonde launch should precede overpass** → sonde near mid-troposphere (~500 hPa) at overpass time (from GRUAN Guide (*)).
2. **Standard ascent rates**:
   ~20' to 500 hPa
   ~45'–60' to 200 hPa (Buehler et al., 2004; Moradi et al., 2010; Seidel et al., 2011)
3. **DL application**: calibration of MWI/ICI onboard **Metop-SGB** and of instruments onboard **Metop-SGA** (+30' delay)

(*) The *GCOS Reference UpperAir Network (GRUAN) GUIDE* https://www.gruan.org/gruan/editor/documents/gcos/gcos-171.pdf

Analysis on GRUAN dedicated launches

Optimal launching time

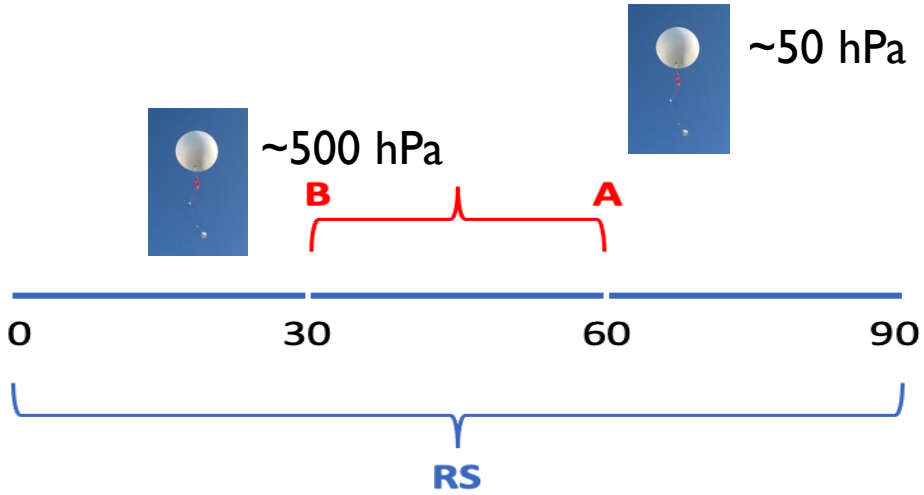

Suggested temporal distance:

- DL approximately **~30'** before the METOP-SGB overpass
- This results in **~60'** between METOP-SGA overpass and the radiosonde launch (the sonde reaching ~50 hPa)

Typical VICIRS tool output

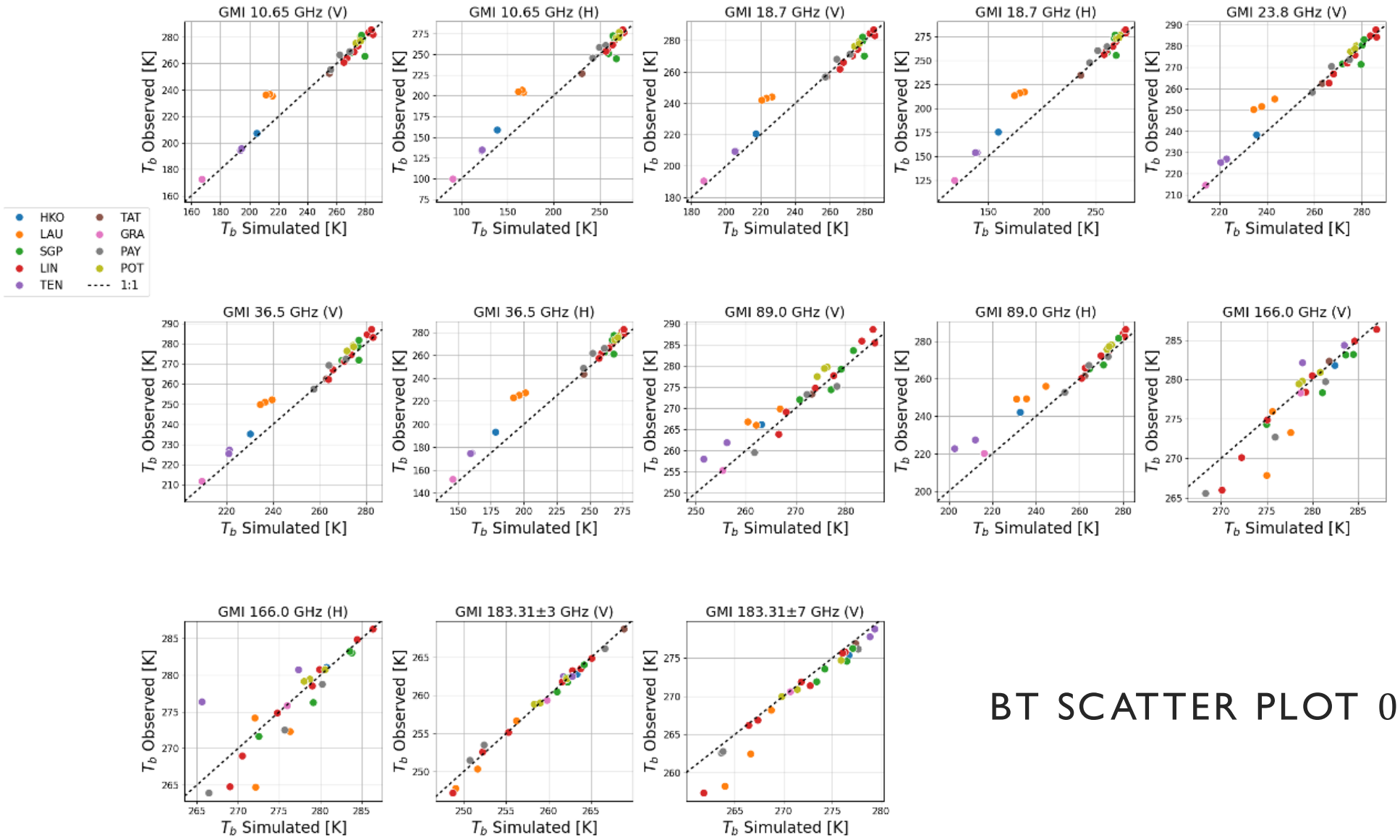

BT SCATTER PLOT $0 \leq \Delta t \leq 30'$

Typical VICIRS tool output

GMI vs RHARM
4-month dataset
(Jan-Apr 2023)

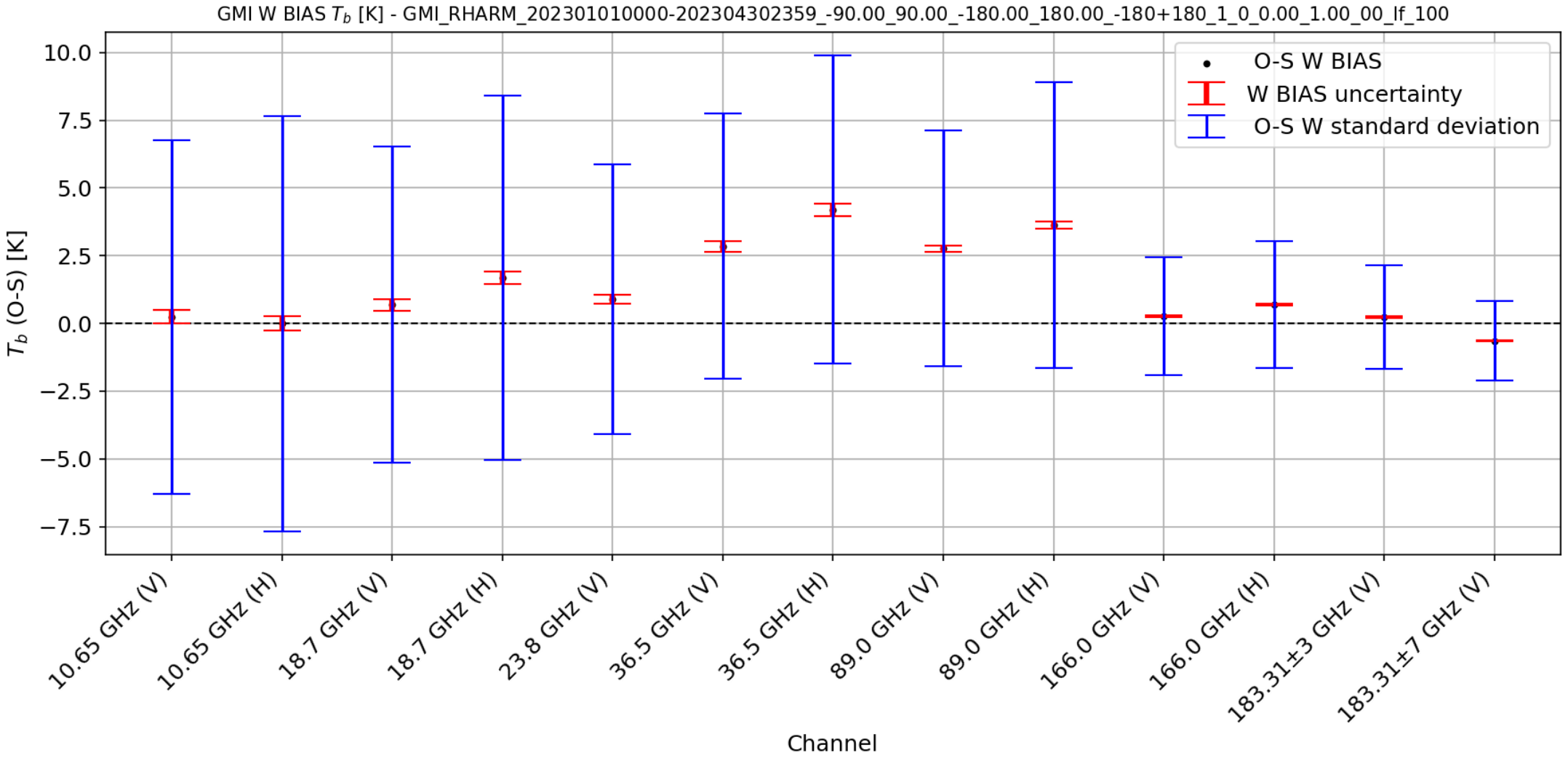

Summary and outlook

- VICIRS tool has been developed
  - Flexible & user friendly
  - Handles GRUAN and RHARM RS
  - Tested with simulated (MWI/ICI) and real (GMI) observations

- Ongoing work
  - Quantification of RS representativeness uncertainty
    - Spatial & temporal representativeness based on NWP
  - Assess overall quality of estimated bias and accuracy
    - vs. RS quantity and quality
  - Exploit VICIRS tool within the post-launch MWI/ICI Cal/Val activities (2026 on)

User feedback for GRUAN

- Sometimes strange values are found
  - e.g., RH > 400% for LIN-RS-01_2_IMS-100-GDP_002_20250107T120000_1-003-001.nc

- Data found in the archive are not always consistent
  - e.g., data search at different times but for the same temporal range may return different match-up lists (at times completely empty)

- How to identify the DL during the validation campaign?
  - Suggestion: attribute **g.Measurement.Comment**: “Copyright xxx EUMETSAT (Contract EUM/CO/XX/XXXXXXX/XXX)”
  - Is this confirmed?
  - Would it be possible to test it before the campaign (e.g., with the remaining DL in Potenza)?

Back-up slides

Spatial & temporal RS representativeness

Statistical approach: *S(r)* modeled with simple step-wise functions

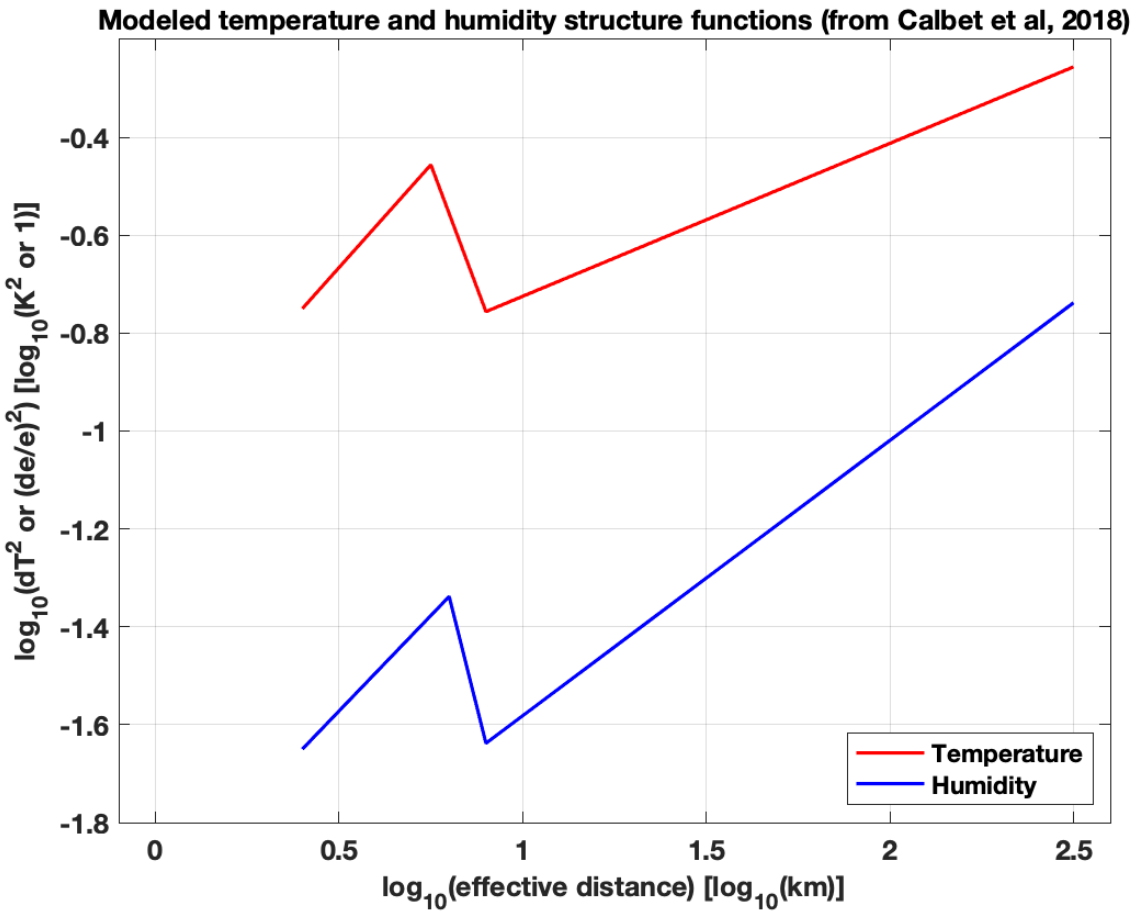

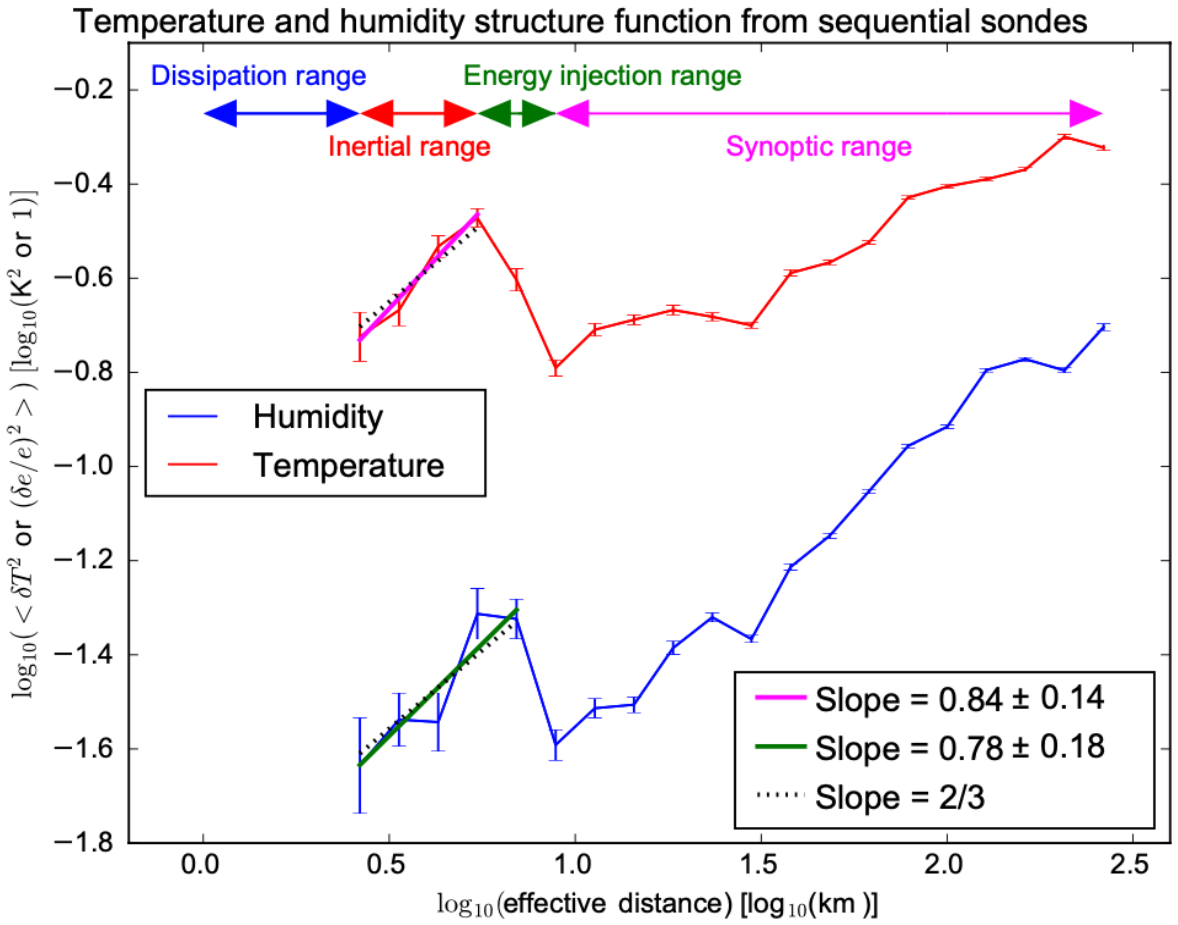

Extension of methodology for uncertainty analysis

RS representativeness: statistical approach (no NWP)

- From lat/lon → distance → $EC_T(r)$ & $EC_e(r)$ → σ_T(h) & σ_e(h)

RS: LIN RS41 GDP 20190226 1200

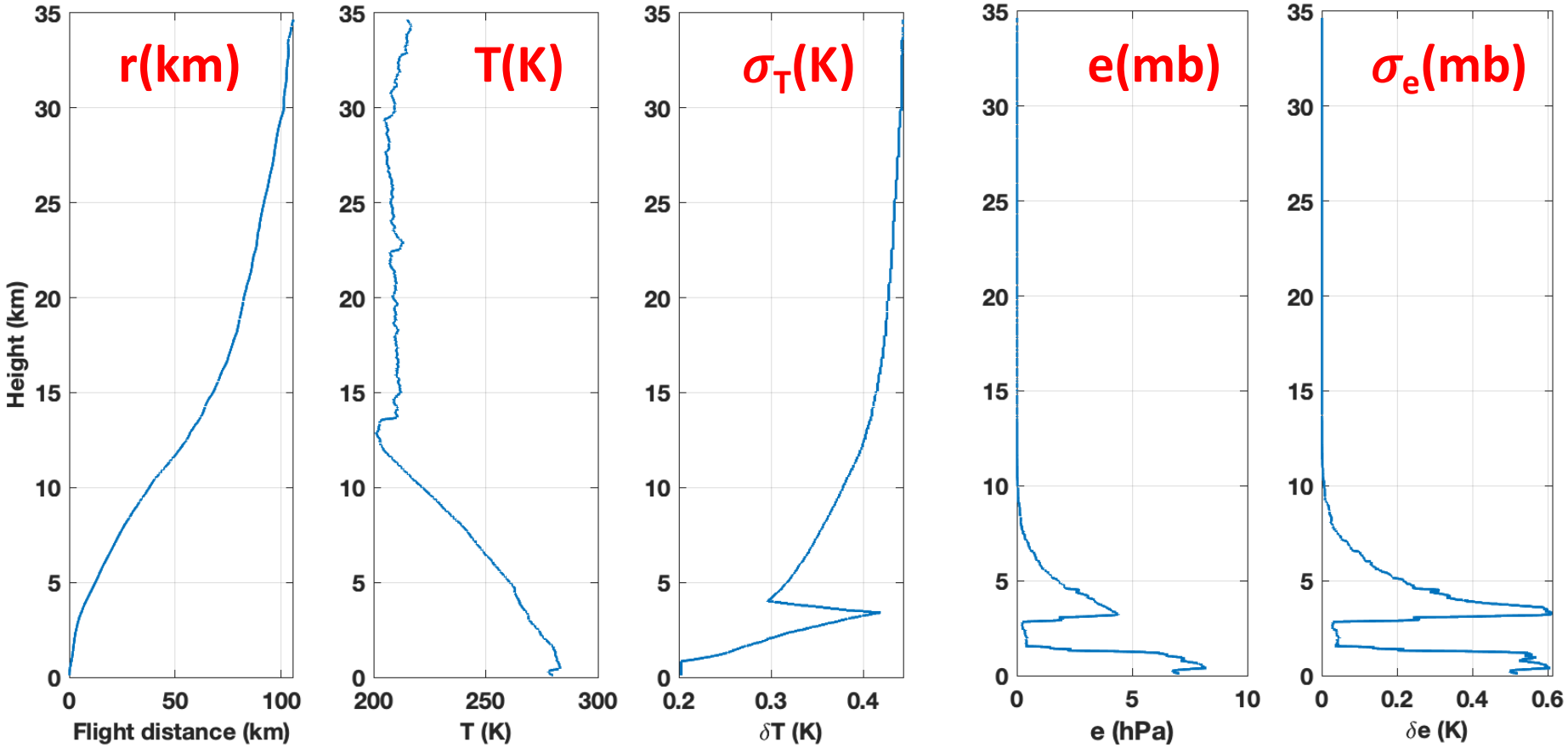

Review of uncertainty sources

- Instrument uncertainty
  - Calibration
  - NEΔT
- Radiosonde uncertainty
  - GRUAN
  - RHARM
- Radiative transfer model (RTM) uncertainty
  - Absorption model

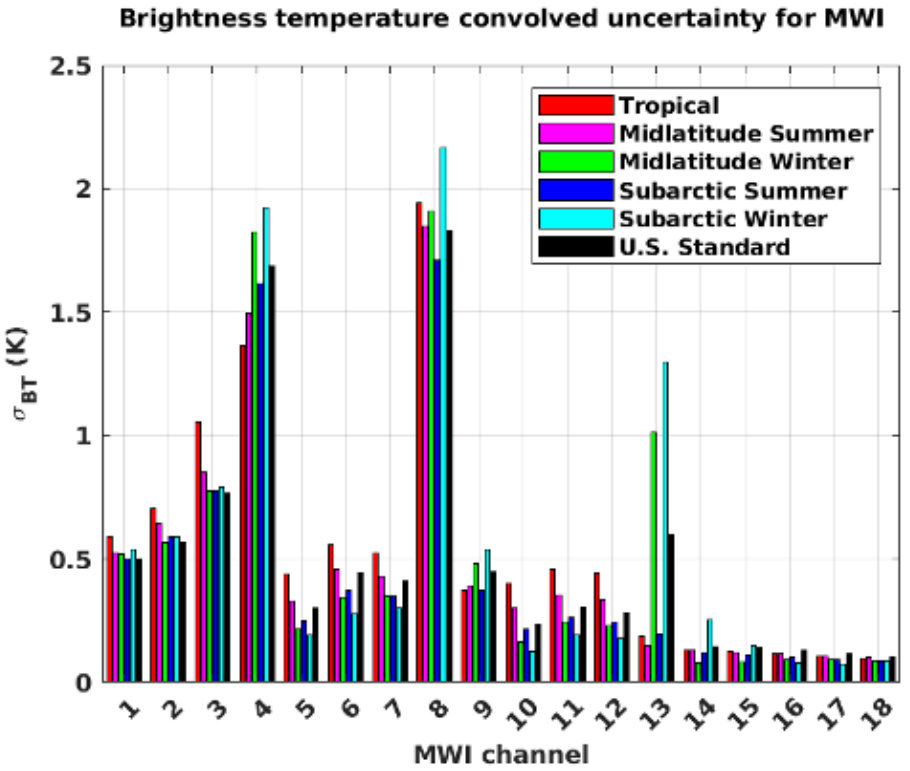

Gallucci et al, ACPD, egusphere-2023-3160

Knowledge gap analysis

Spatial colocation

- Target area (TA) approach[1]
- $u_{BT} = STD(BT_{TA})$
- Circular, RS-driven

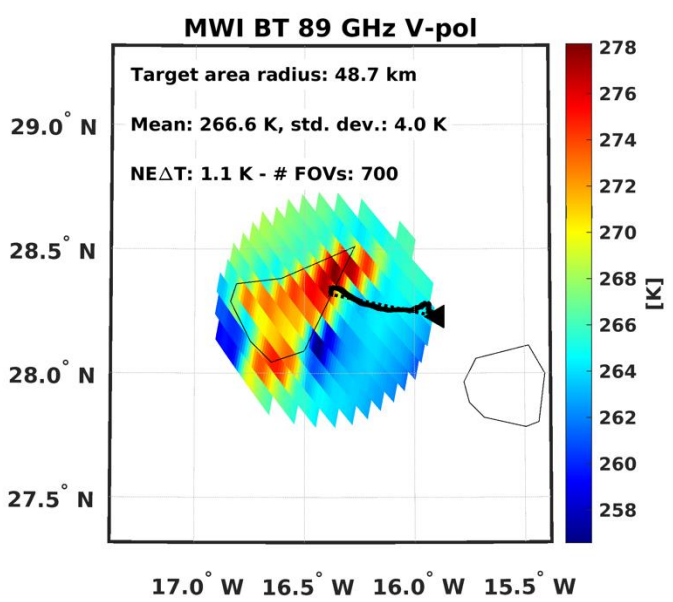

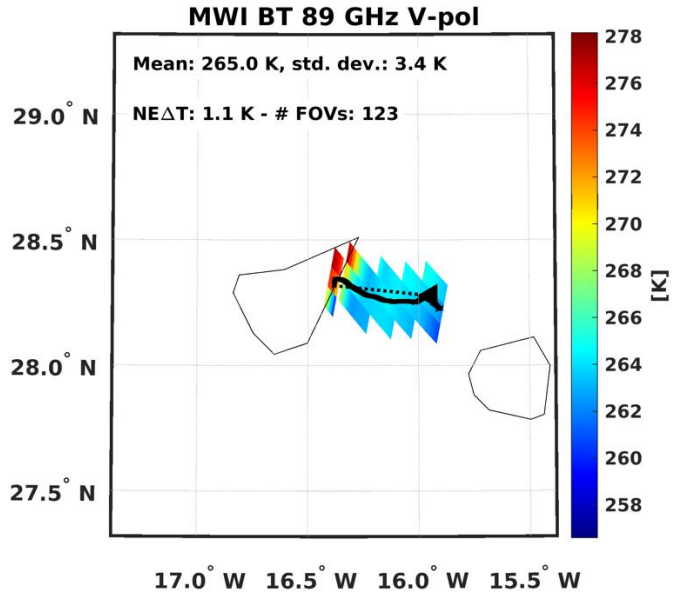

[1]Buehler et al, 2004; Moradi et al, 2010

Knowledge gap analysis

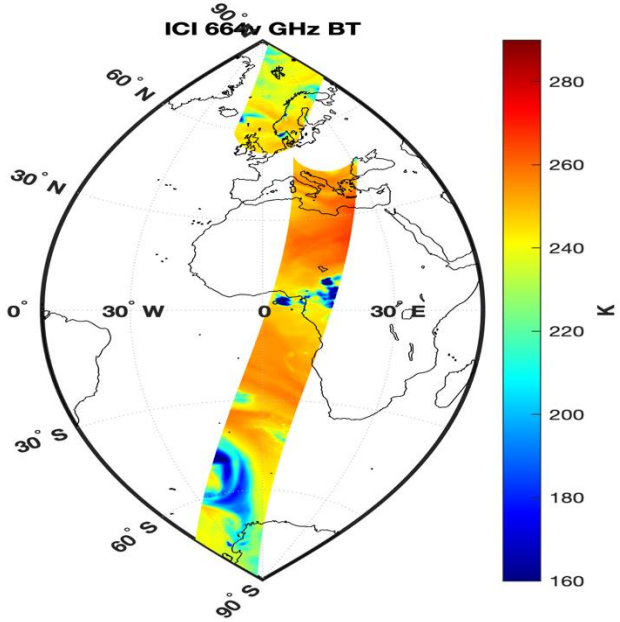

Geolocation

- Analysis based on 183-GHz channels[1]
  - Average geolocation error ~6 km
  - ~113 km^2

- Same order of magnitude of MWI/ICI IFOV distances
  - ~2x9 km (cross-track x along-track)

- u_{GEOL} = STD($BT_{(3x5\text{-}IFOV)}$)
  - ~144 km^2
  - Based on simulated MWI & ICI lev1b data

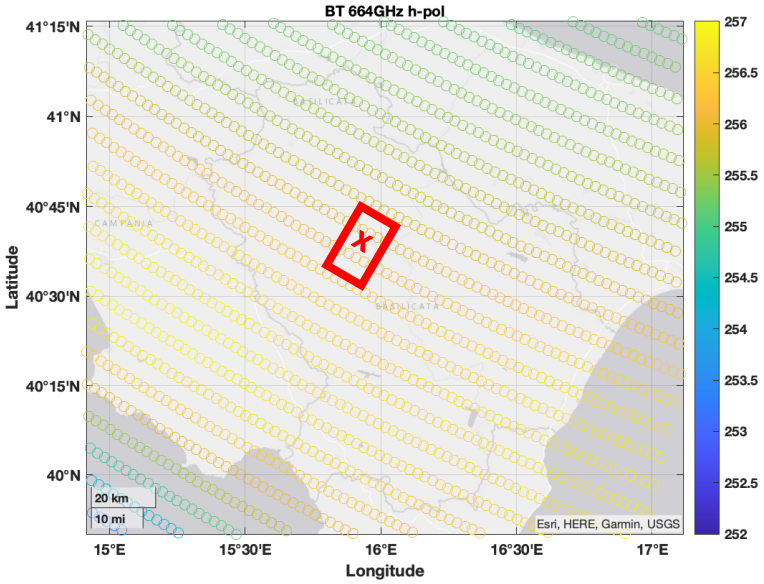

[1]Papa et al, 2021 doi: 10.1109/TGRS.2020.3024677

Knowledge gap analysis

RTM contribution of surface emissivity

- RTM perturbation
- According to land/sea surface uncertainty estimate
  - σ_e = 0.05 (over land) [1]
  - σ_e = 0.018 (over ocean) [2]

From Wang et al. 2017

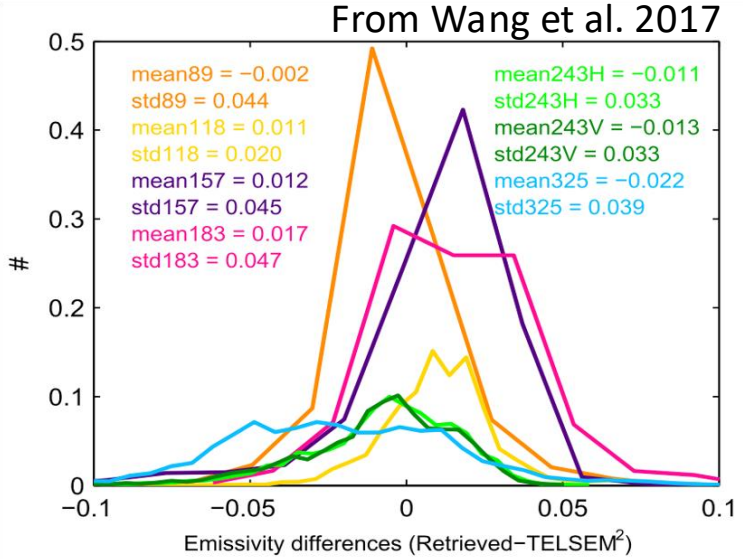

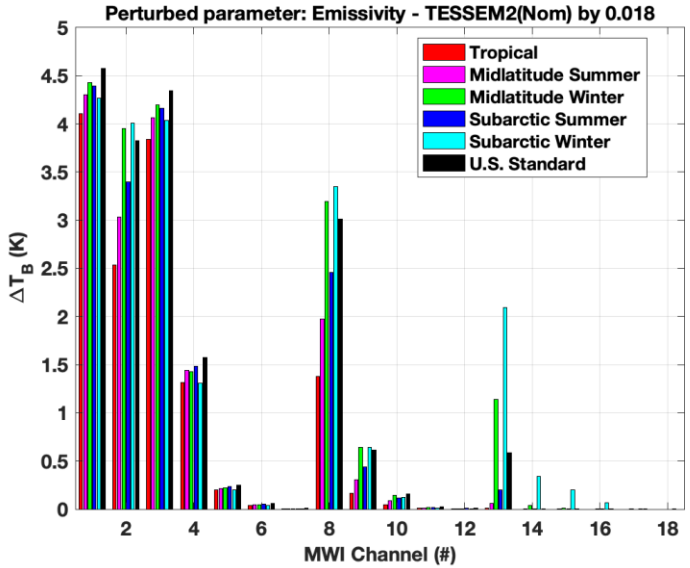

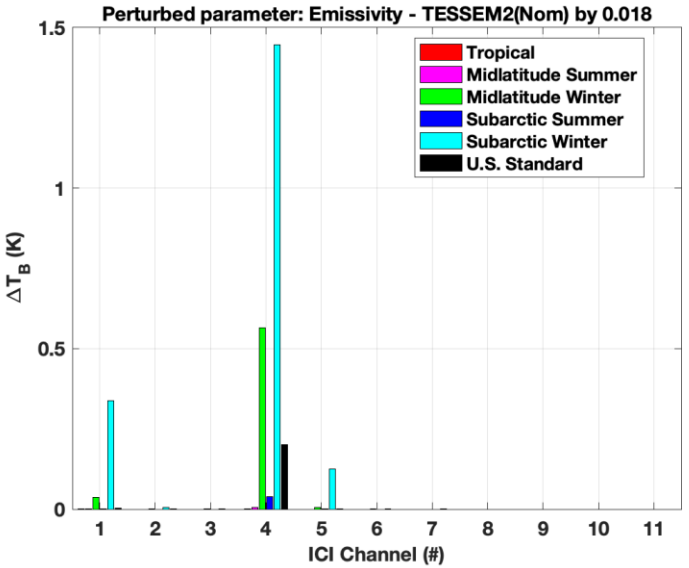

[1]Wang et al. 2017, doi: 10.1175/JTECH-D-16-0188.1
[2]Kilic et al. 2023, doi: 10.1029/2022EA002785

Knowledge gap analysis

RTM contribution of atmospheric model

- RTM optimization[1]
  - Fast parameterized (RTTOV) vs. accurate line-by-line (LBL)
  - RTTOV vs LBL BT
    - diverse 83 profile set and six zenith angles
- Vertical interpolation[2]
  - Discrete levels vs. dense atmosphere
  - $N_{user\ lev} > N_{coef\ lev}$
  - Adapted to MWI/ICI from ATMS channels

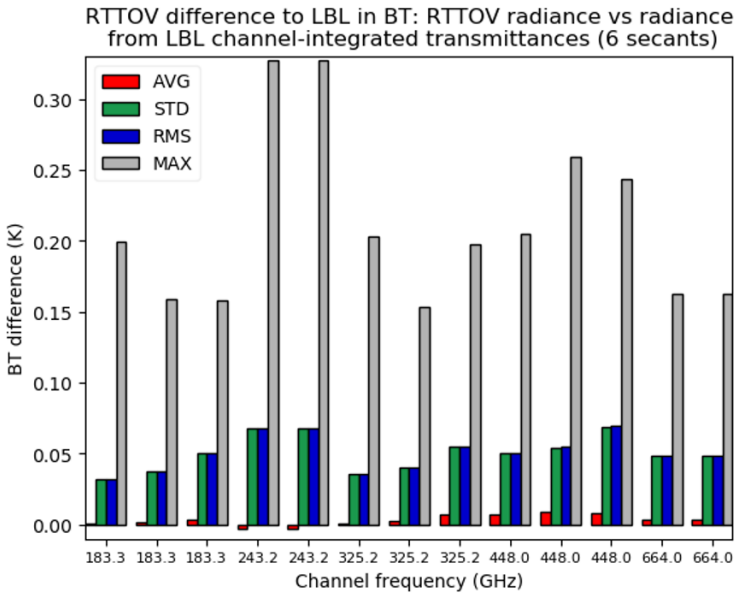

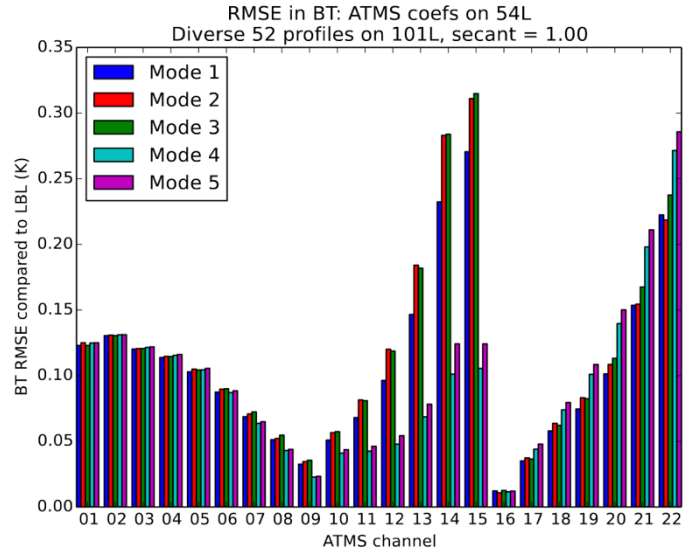

[1]Hocking, NWPSAF, LBL vs RTTOV v13
[2]Hocking 2014, NWPSAF Techl Rep No: 590

Uncertainty due to vertical interpolation

- MWI (using ATMS O2 channels)

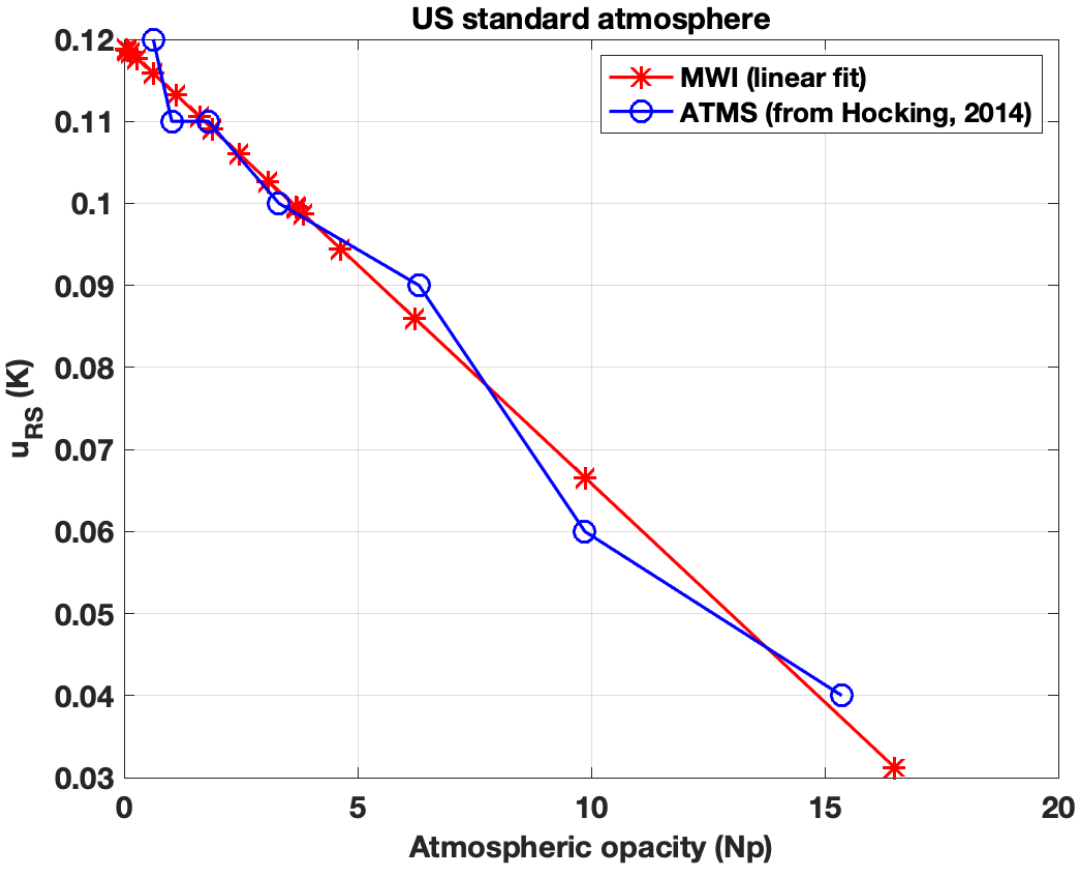

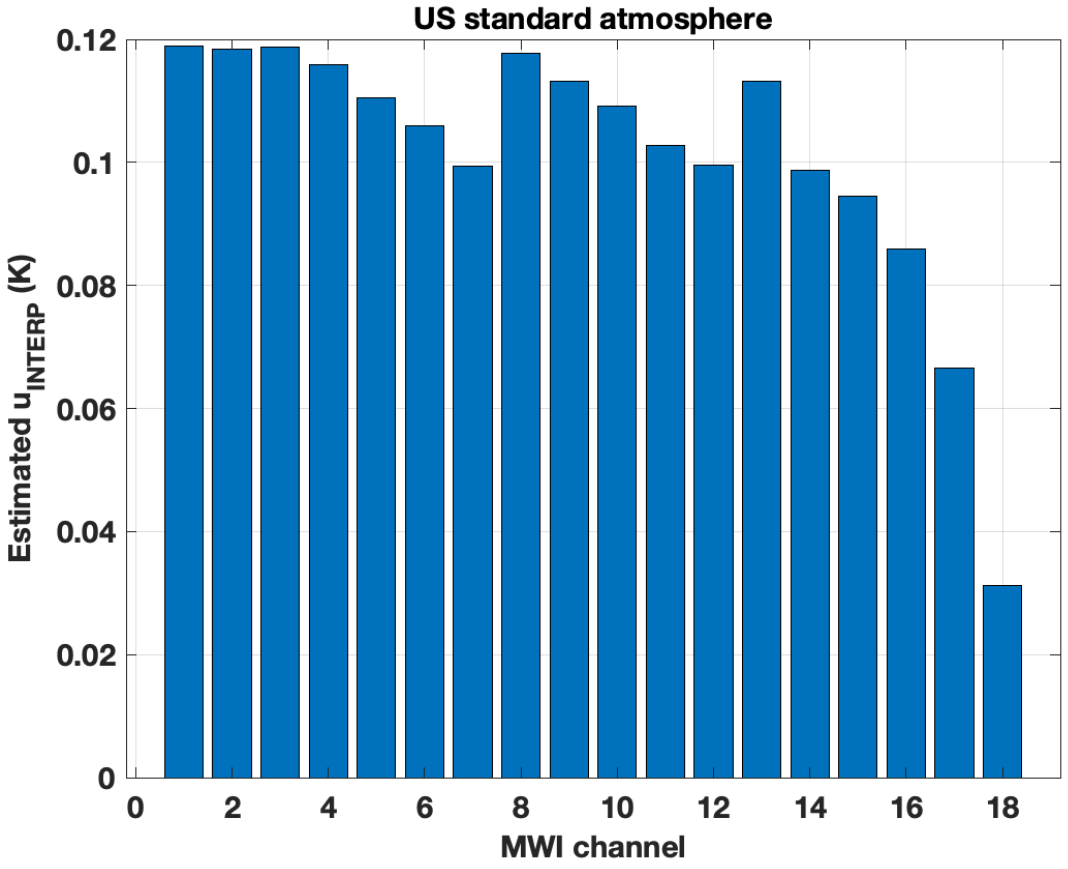

Uncertainty due to vertical interpolation

- ICI (using ATMS WV channels)

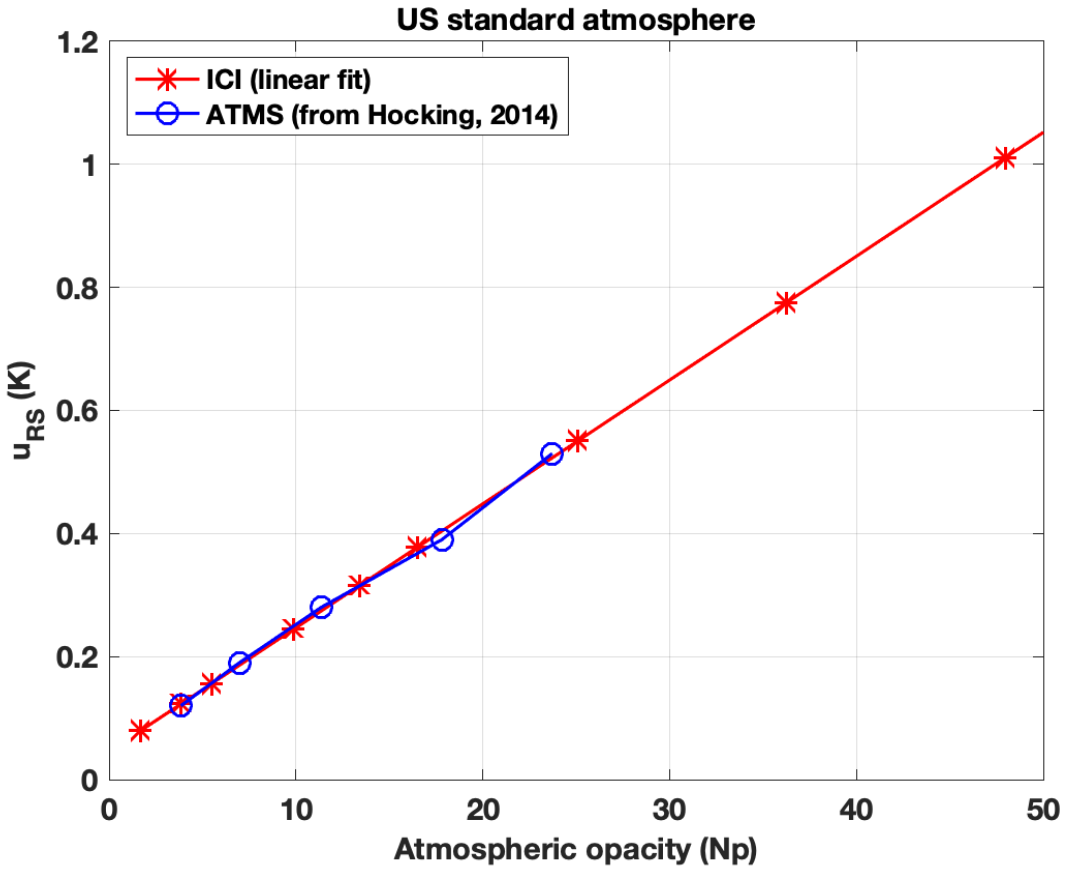

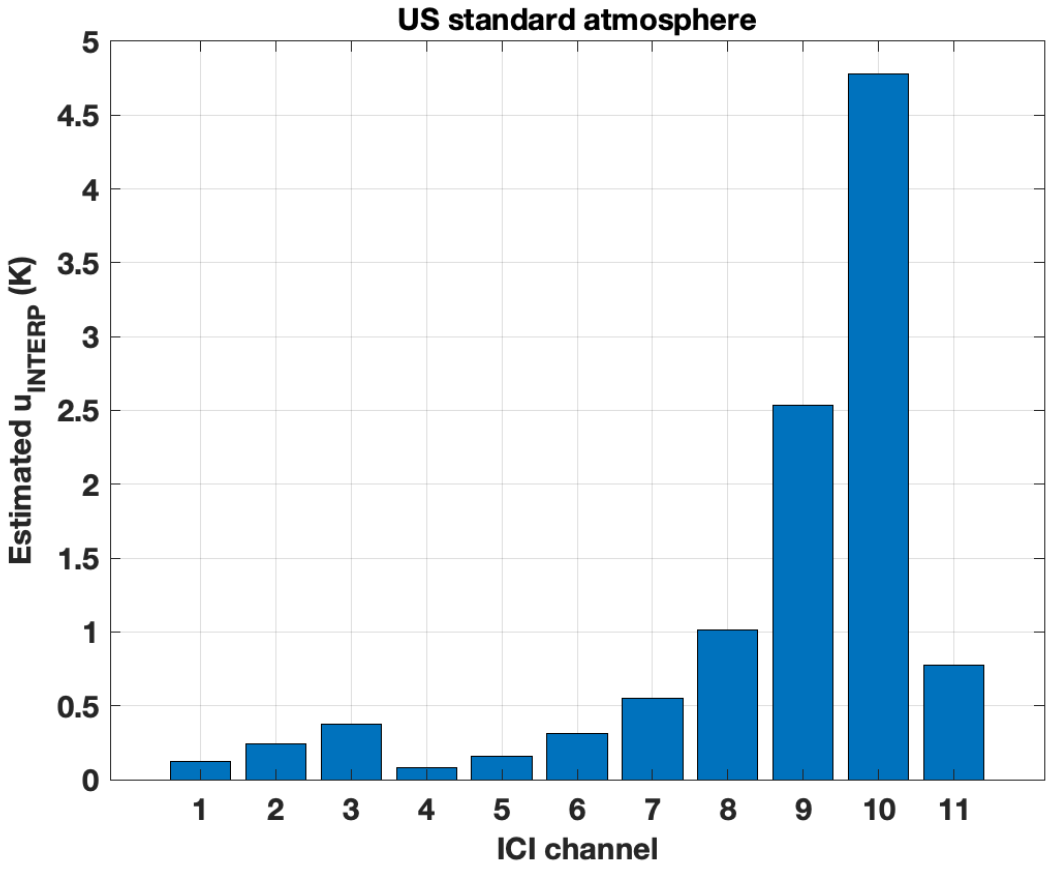

Colocation analysis

FROM: Analysis of GRUAN METOP-SG-B1 MWI/ICI matchup statistics: executive summary

Tropical sites

Table A3. Summary of matchup results in 2022 for GRUAN tropical sites. From left to right: site name and RS type; number of RS launches; number of matchups within +/- 3h (MU@3h) and percentage of RS in cloudy conditions; number of matchups within +/- 1h (MU@1h) and percentage of RS in cloudy conditions; number of matchups within -15/+45min (MU@15') and percentage of RS in cloudy conditions; UTC time of RS operational launches (OP RS); suggested local time for dedicated launches (DL LT); site coordinates; site climatology.

SITE	LAUNCHES (2022)	MU@3h (*)	CLOUDY %	MU@1h (*)	CLOUDY %	MU@15' (*)	CLOUDY %	OP RS (UTC)	DL (LT)	LAT LON	NOTE
HKO RS-41	354	176 (176)	71.0 (125)	0	-	0	-	00-06-12	10-22	22.30° 114.17°	Tropical, urban, low altitude
MTS IMS-100	728	452 (450)	55.55 (250)	308 (308)	55.19 (170)	209 (209)	54.76 (114)	00-12	09-20	24.29 153.98°	Midlat, marine, low altitude
PMO RS-41	66	18 (17)	82.3 (14)	0	-	0	-	15-21	09-22	5.81° -55.21°	Tropical, rural, low altitude
SNG RS-41	17	8 (7)	71.4 (5)	0	-	0	-	00	10-22	1.30° 103.80°	Tropical, urban, low altitude
SNG IMS-100	649	363 (361)	76.73 (277)	-	-	-	-	00	09-22	1.30° 103.80°	Tropical, urban, low altitude
TAT RS-41	341	229 (228)	43.4 (99)	217 (216)	42.6 (92)	124 (123)	39.0 (48)	00-12	09-21	36.06° 140.13°	Subtropical, urban, low altitude
TAT IMS-100	143	97 (95)	43.16 (41)	93 (91)	43.96 (40)	54 (52)	42.31 (22)	00-12	09-21	36.06° 140.13°	Subtropical, urban, low altitude
TEN RS-41	755	481 (479)	36.5 (175)	412 (410)	35.6 (146)	317 (315)	36.65 (115)	00-12	10-21	28.32° -16.38°	Subtropical, rural, mid altitude

(*) the total count of unique matchups is in parentheses

Updated number of needed RS matchups

Instrument Channel	Frequency (GHz)	Bias Req (K)	Bias Unc Req. uB (k=2) Threshold	Breakthru	Objective	TA Sample size (km)	50 inter-sample sep	km inter-scan sep	Assumed square sample /TA	NEDT/ sample	u1 NEDT/TA	u2 uSpec	uEmis	uRAOB	sigma REP 1	Spatial col	Geoloc	uCOL	uTOT	uTOT Carmin.	N = #Sondes for Req. Bias Unc Threshold	Breakthru	Objective
MWI-01	18.7	1.0	0.6	0.3	0.2	50	2.5	9.0	111	2.4	0.2	0.5	4.0	1.7	1.5	0.4	0.5	0.6	4.6		237	948	2132
MWI-02	23.8	1.0	0.6	0.3	0.2	50	2.5	9.0	111	1.7	0.2	0.6	4.0	1.6	1.5	0.3	0.5	0.6	4.6	4.5	236	944	2125
MWI-03	31.4	1.0	0.6	0.3	0.2	30	2.5	9.0	111	2.1	0.2	0.8	4.0	1.7	1.5	0.4	0.6	0.7	4.7	4.6	241	965	2172
MWI-04	50.3	1.0	0.6	0.3	0.2	30	2.5	9.0	111	1.9	0.2	1.7	2.0	1.2	1.5	0.5	0.2	0.5	3.2	3.3	117	467	1050
MWI-05	52.61	1.0	0.6	0.3	0.2	30	2.5	9.0	111	1.9	0.2	0.3	0.1	0.6	1.5	0.5	0.1	0.5	1.6	1.6	30	121	272
MWI-06	53.24	1.0	0.6	0.3	0.2	30	2.5	9.0	111	1.3	0.1	0.4	0.1	0.3	1.5	0.2	0.0	0.2	1.6	0.6	28	112	252
MWI-07	53.75	1.0	0.6	0.3	0.2	30	2.5	9.0	111	1.3	0.1	0.4	0.1	0.2	1.5	0.1	0.0	0.1	1.6	0.1	27	109	245
MWI-08	89	1.0	0.6	0.3	0.2	10	2.5	9.0	111	0.6	0.1	1.9	3.0	1.5	1.5	0.6	0.5	0.8	4.1	4.1	189	757	1704
MWI-09	118.7503±3.2	1.0	0.6	0.3	0.2	10	2.5	9.0	111	1.8	0.2	0.4	0.1	0.2	1.5	0.7	0.2	0.7	1.6	0.1	28	112	253
MWI-10	118.7503±2.1	1.0	0.6	0.3	0.2	10	2.5	9.0	111	2.1	0.2	0.2	0.1	0.2	1.5	0.4	0.1	0.4	1.6	0.1	27	107	242
MWI-11	118.7503±1.4	1.0	0.6	0.3	0.2	10	2.5	9.0	111	2.0	0.2	0.3	0.1	0.3	1.5	0.2	0.0	0.2	1.6	0.1	28	111	249
MWI-12	118.7503±1.2	1.0	0.6	0.3	0.2	10	2.5	9.0	111	2.0	0.2	0.3	0.1	0.4	1.5	0.1	0.0	0.1	1.6	0.2	28	112	251
MWI-13	165.5±0.75	1.0	0.6	0.3	0.2	10	2.5	9.0	111	1.3	0.1	0.6	2.0	1.0	1.5	0.6	0.4	0.7	2.8	2.8	84	338	759
MWI-14	183.31±7.0	1.0	0.6	0.3	0.2	10	2.5	9.0	111	1.1	0.1	0.2	0.2	0.7	1.5	0.5	0.3	0.5	1.7	1.7	31	125	282
MWI-15	183.31±6.1	1.0	0.6	0.3	0.2	10	2.5	9.0	111	1.3	0.1	0.1	0.2	0.7	1.5	0.4	0.3	0.5	1.7	1.7	31	125	282
MWI-16	183.31±4.9	1.0	0.6	0.3	0.2	10	2.5	9.0	111	1.3	0.1	0.1	0.0	0.7	1.5	0.5	0.3	0.5	1.7	1.7	31	125	281
MWI-17	183.31±3.4	1.0	0.6	0.3	0.2	10	2.5	9.0	111	1.3	0.1	0.1	0.0	0.8	1.5	0.5	0.2	0.5	1.7	2.0	32	130	292
MWI-18	183.31±2.0	1.0	0.6	0.3	0.2	10	2.5	9.0	111	1.3	0.1	0.1	0.0	0.9	1.5	0.5	0.2	0.5	1.8	2.3	35	141	317
ICI Average V-channels			0.6	0.3	0.2				103	1.3	0.1	0.2	0.0	0.9	1.5	0.5	0.4	0.6	1.8	2.1	34	137	308
ICI-01	183.31±7.0	1.0	0.6	0.3	0.2	16	2.7	9.0	103	0.9	0.1	0.1	0.2	0.7	1.5	0.4	0.3	0.5	1.7	1.7	31	125	281
ICI-02	183.31±3.4	1.0	0.6	0.3	0.2	16	2.7	9.0	103	1.1	0.1	0.1	0.0	0.8	1.5	0.5	0.2	0.5	1.7	2.0	32	130	292
ICI-03	183.31±2.0	1.0	0.6	0.3	0.2	16	2.7	9.0	103	1.0	0.1	0.1	0.0	0.9	1.5	0.4	0.2	0.4	1.8	2.3	35	141	316
ICI-04	243.2±2.5	1.5	0.6	0.3	0.2	16	2.7	9.0	103	0.8	0.1	0.6	0.0	1.0	1.5	0.4	0.6	0.7	1.9	2.8	40	158	356
ICI-04H	243.2±2.5	1.5	0.6	0.3	0.2	16	2.7	9.0	103	0.9	0.1	0.2	0.9	1.0	1.5	0.3	0.6	0.7	2.0	2.8	45	180	404
ICI-05	325.15±9.5	1.5	0.6	0.3	0.2	16	2.7	9.0	103	1.4	0.1	0.1	0.1	0.7	1.5	0.6	0.6	0.8	1.7	1.7	31	124	279
ICI-06	325.15±3.5	1.5	0.6	0.3	0.2	16	2.7	9.0	103	1.4	0.1	0.1	0.0	0.8	1.5	0.6	0.4	0.7	1.7	2.0	33	130	293
ICI-07	325.15±1.5	1.5	0.6	0.3	0.2	16	2.7	9.0	103	1.6	0.2	0.1	0.0	0.9	1.5	0.6	0.3	0.6	1.8	2.3	35	142	319
ICI-08	448±7.2	1.5	0.6	0.3	0.2	16	2.7	9.0	103	1.3	0.1	0.1	0.0	0.7	1.5	0.6	0.4	0.7	1.7	1.7	31	125	282
ICI-09	448±3.0	1.5	0.6	0.3	0.2	16	2.7	9.0	103	1.5	0.1	0.1	0.0	0.8	1.5	0.6	0.2	0.6	1.7	2.0	33	131	294
ICI-10	448±1.4	1.5	0.6	0.3	0.2	16	2.7	9.0	103	2.0	0.2	0.2	0.0	0.9	1.5	0.4	0.1	0.4	1.8	2.3	36	143	321
ICI-11	664±4.2	1.5	0.6	0.3	0.2	16	2.7	9.0	103	1.5	0.1		0.0	1.1	1.5	0.6	0.5	0.8	1.9	2.0	39	156	351
ICI-11H	664±4.2	1.5	0.6	0.3	0.2	16	2.7	9.0	103	1.4	0.1		0.0	1.1	1.5	0.6	0.6	0.8	1.9	2.0	39	156	351
Source												ISMAR Final Report Figure 28	VICIRS 0.05 e_sigma, TESSEM2, Mean 53° nominal	Carminati et al, 2019 Figure 4	Bormann & Bauer, 2010 Fig 3+9	VICIRS study, based on MWI/ICI simulated l1c & RHARM (65 matchup	VICIRS study, based on Papa et al., 2021 (for 2-pol chans, it shows V-pol)	TOT of colocation error from VICIRS study	uTOT^2= NEDT^2+ uSpec^2 +uEmis^ 2+uRAOB ^2+uREP ^2	Carminati et al, 2019 Figure 6	Black = Good channel match Grey = Approx Channel match		

The metrological approach

- GRUAN
  - Immler et al. 2010
  - VIM
  - GUM

$\varepsilon = m_1 - m_2$ Error

u_1 Random uncertainty of m_1

u_2 Random uncertainty of m_2

σ Uncertainty of matching

(1-σ level)

Consistency check between two measurements (m_1 and m_2)

$$|m_1 - m_2| < k\sqrt{\sigma^2 + u_1^2 + u_2^2}$$

k: coverage factor

From Immler et al., 2010

$\lvert m_1 - m_2 \rvert < k\sqrt{\sigma^2 + u_1^2 + u_2^2}$	TRUE	FALSE	significance level
$k=1$	consistent	suspicious	32%
$k=2$	in agreement	significantly different	4.5%
$k=3$	–	inconsistent	0.27%

Analysis on GRUAN dedicated launches

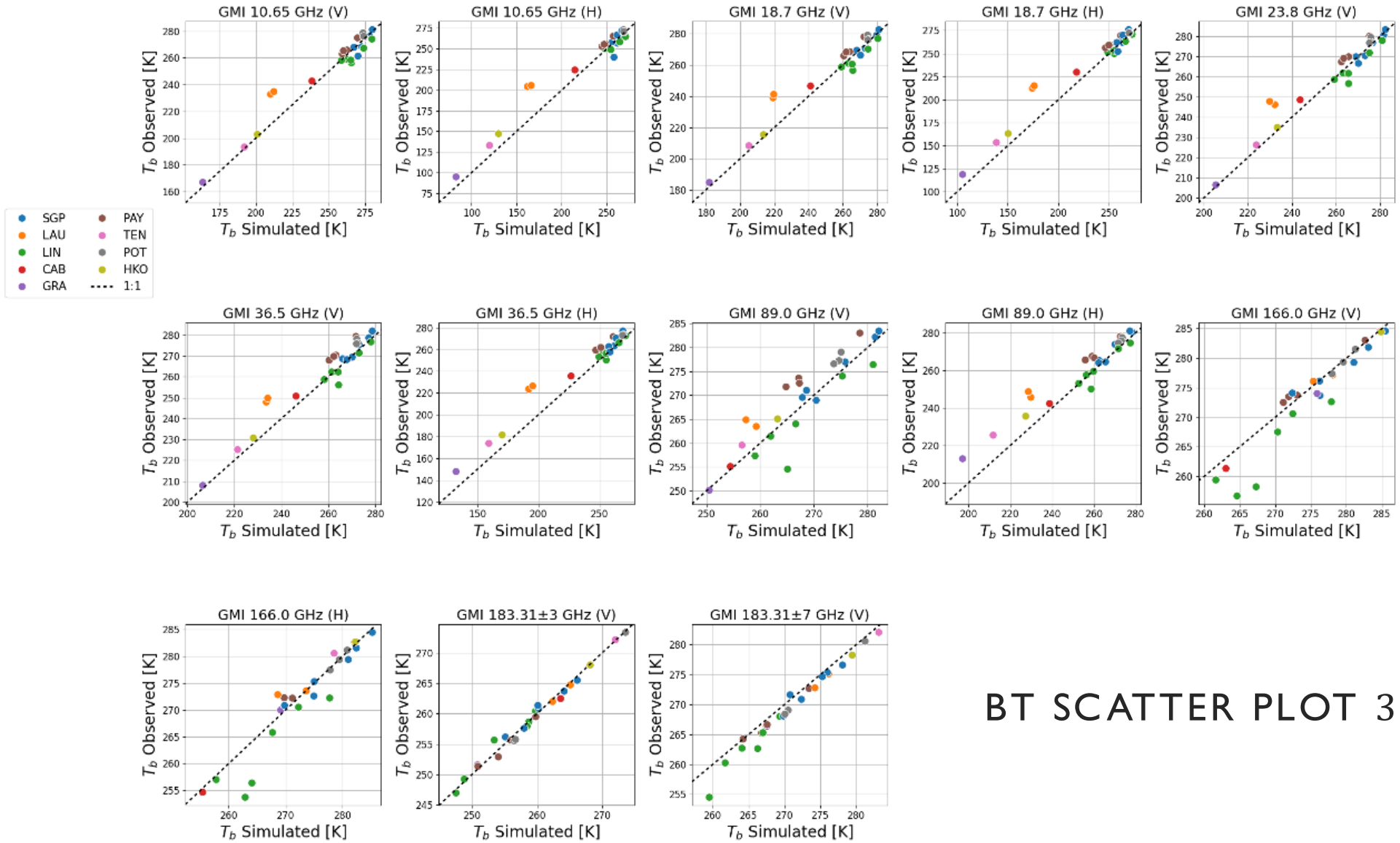

BT SCATTER PLOT $30' < \Delta t \leq 60'$

Analysis on GRUAN dedicated launches